INSTITUTE OF BIOCHEMISTRY
SWISS FEDERAL INSTITUTE OF TECHNOLOGY ZURICH

Investigation of Caveolar Endocytosis by TIRF Microscopy

Diploma Thesis

Rolf Suter
January–June 2005

This work was done under the supervision of Helge Ewers
in the laboratory of Prof. Dr. Ari Helenius

Abstract

Here, we present a detailed study of endocytic internalization of caveolae. The use of total internal reflection fluorescence (TIRF) microscopy combined with the expression of caveolin 1-GFP variants allowed us to visualize single endocytic events at the plasma membrane with a high spatial and temporal resolution.

We developed a quantitative fluorescence-microscopy assay based on computational image analysis. When the internalization of caveolae was graphed as loss in fluorescence-intensity upon exit from the evanescent field, a time-constant of $\tau = 0.4\,\mathrm{s}$ was yielded.

To find factors involved in caveolar endocytosis, we coexpressed GFP-tagged variants of proteins involved in nucleation of actin polymerization and/or signaling with caveolin 1-mRFP to follow the internalization of caveolae in respect to these markers. We rationalized, that interaction partners would transiently colocalize with caveolin 1-mRFP labeled caveolae close in time to the uptake of an individual caveolae. While all constructs used were found to localize to individual caveolae at some point, none of them did so in the majority of internalizing caveolae in a cell.

In order to specifically image triggered endocytic events, we added fluorescently labeled cholera toxin B to live cells. Soon after binding, we could observe internalization of cholera toxin in caveolin 1-positive vesicles. The vesicles distinguished in this way were easier to follow than overall caveolae in untreated cells. By combining epi- and TIR-fluorescence microscopy we were able to follow internalizing vesicles into the cell. The signaling molecule phosphatidylinositol-4,5-bisphosphate (PIP_2) detected via a PIP_2 binding PH-domain fused to GFP could occasionally be detected in cholera toxin internalizing caveolae.

Overall, we successfully established a microscopy-based assay that yields quantitative data. Much more time will be required to analyze the gathered imaging data in full. Our work pushes into a gap in the endocytic field just at a time, at which factors involved in caveolar endocytosis became identified by a genome-wide screen by Pelkmans et al [1]. Combined with information about certain interactors of caveolin from this screen, the continuation of our work will help to elucidate early events in caveolar endocytosis.

Contents

1 Introduction

1.1 Endocytosis

Nearly all eukaryotic cells use the process of endocytosis to capture extracellular molecules by enclosure within membrane vesicles or vacuoles derived from the plasma membrane. Cells use endocytosis to take up nutrients, defend themselves against pathogens and to maintain homeostasis. However, some toxins, viruses and other pathogens abuse the endocytic pathways to enter the host cell. At least five different pathways of endocytosis exist. Phagocytosis and macropinocytosis are used to engulf large particles and large amounts of fluid respectively. In contrast, clathrin-coated vesicles, non-clathrin-coated vesicles and caveolae are small and used to ingest fluids and solutes.

1.1.1 Clathrin-Mediated Endocytosis

Clathrin-dependent endocytosis is a receptor-mediated process, which begins at clathrin-coated pits. These occupy approximatly 2 % of the total plasma membrane. Receptor-ligand complexes either induce the formation of new clathrin-coated pits or laterally move into preexisting ones. These pits consist of clathrin triskelions and adapter proteins. Clathrin is a protein complex with a three-legged structure composed of three heavy chains with light chains tightly associated to each. Adaptor or assembly proteins (AP) are responsible for targeting and transport specificity. There are at least four different AP complexes that each consist of four different polypeptides.

The pinching off from the plasma membrane to form clathrin-coated vesicles requires the GTPase dynamin. Dynamin self assembles around the neck of the pits. Dynamin binds to the lipid phosphatidylinositol-4,5-bisphosphate (PIP_2). This allows regulation of dynamin [2] and the association of dynamin with membranes [3].

The actin cytoskeleton plays an important role in clathrin-mediated endocytosis [4, 5, 6]. The actin-related protein 3 (Arp3), which belongs to the actin-nucleating Arp2/3-complex, is transiently recruited to internalizing clathrin coated structures [5]. The filamentous actin (F-actin) binding protein cortactin is a component of clathrin-coated pits which is also involved in endocytosis [7]. Dynamin interacts through its proline/arginine-rich domain (PRD) with the Src homology 3 (SH3) domain of cortactin [8].

After leaving the plasma membrane, the clathrin-coated vesicles, which share their structure with a soccer ball, rapidly shed their coat.

1.1.2 Caveolar Endocytosis

Caveolae are flask-shaped invaginations of the plasma membrane that were first discovered by electron microscopy due to their characterisic morphology. Their typical size is about 50–80 nm. Caveolae are present in many cell types and are involved in endocytosis and maintainance of cellular cholesterol levels, but also other processes. Caveolae are enriched in cholesterol, glycosphingolipids and glycosylphosphatidylinositol (GPI) anchored proteins. The coat of the caveolar invaginations and vesicles is formed by self-

assembly of the integral membrane protein caveolin 1 with low amounts of the caveolin 2 isoform.

Caveolin Caveolin 1 belongs to an evolutionary conserved family of 21–24 kDa proteins. It has an unusual typology in that it has a cytosolic N- and C-terminal domain, connected by a hydrophobic sequence, which is embedded in the plasma membrane, but does not span it. Caveolin 1 can form dimers and higher oligomers and binds cholesterol with high affinity [9].

Caveolin 1 is triply palmitoylated by the linkage of 16-carbon saturated fatty acids by an S-ester to cysteines 133, 143, and 156 near the C-terminus. Palmitoylation of at least two cystein residues is required for cholesterol binding.

Caveolin 1 has a phosphorylation site on tyrosin 14, which is a principal target for Src kinase [10]. Insulin, angiotensin II, endothelin 1 and oxidative stress activate Src family kinases leading to the phosphorylation of caveolin 1 [11, 12].

Factors Involved in Caveolar Endocytosis The study of caveolar endocytosis by the use of Simian virus 40 (SV40) provided evidence for the involvement of actin polymerization, dynamin recruitment and tyrosine phosphorylation in internalization of caveolae [13].

Supporting this idea, ultrastructural and biochemical experiments have shown the implication of the actin cytoskeleton in caveolae function. In addition, the F-actin cross-linking protein filamin was identified as a ligand for caveolin 1 [14].

Despite all these findings, the exact mechanism by which caveolae internalize, and what factors are involved in this process is not well understood.

1.1.3 Clathrin- and Caveolin-Independent Endocytosis

Several other pathways of endocytosis exist. It is difficult to categorize them unambiguously, but the dependence on dynamin and cholesterol are characteristics, that help to classify these pathways. Endocytosis independent of clathrin and caveolin is still poorly understood and under intense investigation.

1.1.4 Hijacking Caveolar Endocytosis

Several bacteria, viruses and toxins have developed mechanisms to abuse the cellular endocytic machinery to invade their host cells. This is also true for the caveolar pathway.

Simian virus 40 is a small nonenveloped DNA virus that belongs to the papovavirus family that replicates in the nucleus. It was the first virus found to enter cells via the caveolar pathway. SV40 binds to surface ganglioside GM1 [15] and moves laterally until trapped in caveolae. Once in a caveola, SV40 induces a signaling cascade that leads to recruitment of dynamin 2 and actin polymerization-propelled internalization of the virus-loaded caveola [13].

Cholera toxin is the causing agent of the disease cholera. It is produced by the bacterium *Vibrio cholerae* and consists of two subunits A and B. While the A subunit

is responsible for pathology, the pentameric B subunit binds to the plasma membrane. It has high affinity and specificity to GM1, the same cell surface receptor as SV40 binds to. After binding to the cell surface, cholera toxin enters the cell mainly by the caveolar pathway to the Golgi apparatus.

1.2 TIRF Microscopy

In order to visualize endocytic events it is useful to selectively look at the plasma membrane. Fluorescence microscopy is a natural choice to trace proteins labeled with a fluorophore within live cells. Conventional fluorescence microscopy illuminates the whole cell. Therefore, all labeled proteins within the cell are excited. It is impossible to distinguish between proteins that are in the cytosol and such that are attached to the plasma membrane. Also, cytosolic fluorescence might overcome the signal localized to the plasma membrane. One microscopy technique that exclusively excites fluorescent molecules within a defined depth in the cell is confocal microscopy. However, even confocal slices which have a depth of 500–1000 nm are to thick to resolve the dynamics of the small endocytic vesicles of a diameter of about 100 nm. Furthermore, confocal microscopy is to slow to resolve the endocytic dynamics and causes fast bleaching of the fluorescent molecules.

Total internal reflection fluorescence (TIRF) microscopy (also called evanescent field fluorescence microscopy) overcomes these problems (for review see [16, 17]). It allows the selective excitation of fluorophores in an aqueous or cellular environment close to a surface of differing refractive index (within ~ 100 nm). Fluorophores farther away from the surface are not excited. This feature of TIRF microscopy allows the study of the endocytic events [4].

1.2.1 Theory of TIRF

The thin layer of illumination is an evanescent field, which forms when a beam of light traveling in a medium with a high refractive index, like glass, (n_{glass}) encounters one of low refractive index such as water (n_{liquid}). When the incident angle θ_c, measured from the normal, is larger than the so called critical angle, the beam undergoes total internal reflection (TIR). This means, that the light does not cross the interface glass/water and is reflected instead. Classical electrodynamics do not allow an electromagnetic wave to dissappear discountinuously at an interface. Therefore, TIR generates a very thin electromagnetic field in the liquid, the evanescent field, which oscillates with the same frequency as the incident light. The intensity of the evanescent field decreases exponentially with the distance to the interface. The critical angle θ_c can be calculated from:

$$\theta_c = \sin^{-1}\left(\frac{n_{liquid}}{n_{glass}}\right) \tag{1}$$

1.2.2 Optical Configurations

In general there are two ways to build up a TIRF microscope. The light, usually from a laser with a total visible ouput in the 100 mW range, which generates the evanescent field can either be directed through a prism to the TIR interface or through a high numerical aperture (NA > 1.4) microscope objective itself (Figure 1).

TIRF with a Prism Using a prism can be an inexpensive and easy way to set up a TIRF microscope. A prism-based TIRF microscope can illuminate a larger area. This can be an advantage when visualizing several cells or cells that are spread over a large area. Depending on the exact configuration, the sample has to be sandwiched into a narrow space between the prism and the objective (Figure 1 a). This makes it difficult to access the sample.

Prismless TIR through the Objective Through-the-objective TIRF microscopes allow free access to the sample. They also give a higher image quality and spatial resolution. However, the illumination is not pure. Scattered light and luminescence from the objective also contribute to the illumination of the sample.

A high incident angle can be achieved when the laser beam is introduced off-axis into the objective (Figure 1 b). The NA of the objective must be substantly greater than n_{liquid}. Using a NA = 1.4 objective and water with $n_{liquid} = 1.33$ the required conditions are fulfilled. But when viewing a cell at $n_{liquid} = 1.38$ the TIR is just above the critical angle which leads to a deep evanescent field. Some dense organelles then would convert some of the evanescent field into scattered light, which gives a poor resolution.

1.3 Aim of this Project

The caveolar pathway of endocytosis has been intensively studied previously (for review see [9]). But up to now less is known about the dynamics of caveolar endocytosis. Also the temporal interplay of endocytic factors during the internalization of caveolae is not well understood.

Earlier work [4, 5] examined the temporal aspects of clathrin-mediated endocytosis using TIRF microscopy. In those studies fluorescently labeled clathrin was imaged together with labeled candidate protein on a TIRF microscope.

The aim of this project is to set up a TIRF microscopy based assay to visualize caveolar endocytosis. Quantitative fluorescence data will be generated and computationally extracted and analyzed to dissect the temporal resolution of caveolae internalization. Furthermore, different potential interaction partners will be co-imaged with caveolae to qualitatively assess their role in caveolar endocytosis.

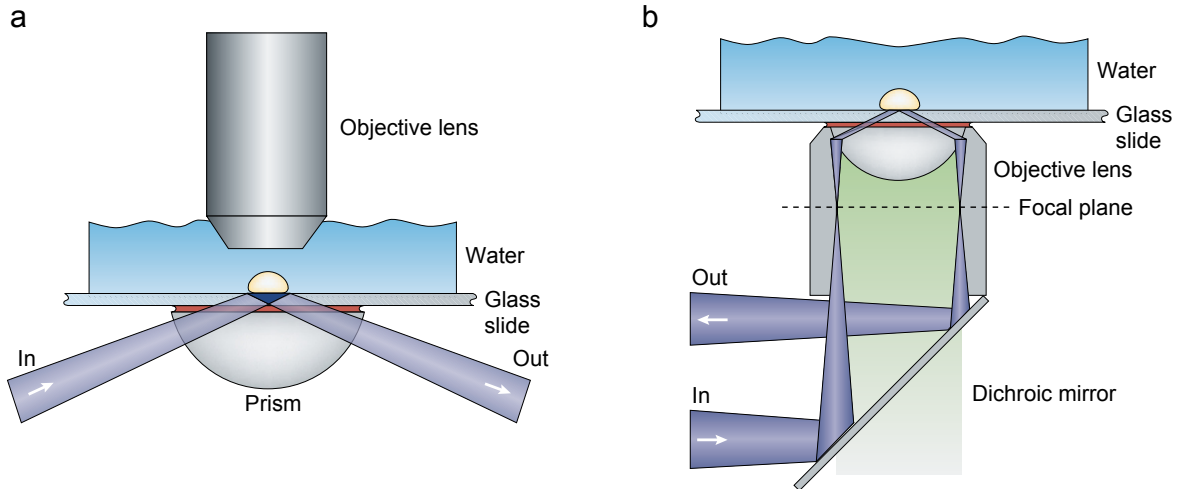

Figure 1: Two types of TIRF microscopes. (a) A prism-type TIRF microscope. (b) Outline of a through-the-objective TIRF microscope.

2 Materials and Methods

2.1 Materials

2.1.1 Media for Cell Culture

CO_2-independent medium	18045-054	Gibco Life Techn.
D-MEM	41965-039	Gibco Life Techn.
MEMα	32561-029	Gibco Life Techn.
Trypsin-EDTA (1×)	25300-054	Gibco Life Techn.

2.1.2 Cells

CV1		ATCC
HeLa		ATCC
HeLa Cav1-mRFP		Arnold Hayer

2.1.3 Plasmids

Arp3-EGFP		Matt Welch
Cav1-EGFP		Thomas Bürli
Cav1-mRFP		Thomas Bürli
Cttn-EGFP		Rolf Suter
Dyn2-EGFP		Hong Cao [18, 19]
EGFP-actin	6116-1	Clontech
GFP-Grb2		Niki Scaplehorn [20]
PH-PLC-EGFP		Pietro de Camili
YFP-dSH2		Stefan Moese

2.1.4 Kits for Transfection

Cell Line Nucleofector Kit R	VCA-1001	Amaxa
Cell Line Nucleofector Kit V	VCA-1003	Amaxa

2.1.5 Others

Cholera toxin subunit B, AF647	C-34778	Molecular Probes
Geneticin (G-418 Sulphate)	11811-031	Gibco Life Techn.
HEPES	H4034	Sigma
HEPES Buffer Solution 1M	15630-056	Gibco Life Techn.
Sodium Orthovanadate (Na_3VO_4)	567540	Calbiochem

2.2 Equipment

2.2.1 TIRF Microscope

Inverted Microscope	IX-71	Olympus
PlanApo 60×/1.45 Oil objective		Olympus
Kr-Ar laser	2060-RS	Spectra Physics
TIRF setup		TILL Photonics
CCD Camera	Imageo-QE	TILL Photonics

2.3 Software

TILLvisION 4.0	TILL Photonics
ImageJ 1.33	NIH
Excel	Microsoft
Kaleidagraph	Synergy Software
Photoshop	Adobe

2.4 Methods

2.4.1 Cell Culture

HeLa Cells HeLa cells were obtained from the American Type Culture Collection (ATCC). The HeLa Cav1-mRFP cells stably expressing caveolin 1-monomeric red fluorescent protein (caveolin 1-mRFP) were produced by Arnold Hayer. Cells were maintained in 10-cm Petri dishes at 5 % CO_2 and 37 °C in MEMα supplemented with 10 % fetal calf serum (FCS), 1× nonessential amino acids (NEAA) and 50 mM HEPES. To keep the HeLa Cav1-mRFP cells under selective pressure, 100 μl of a geneticin solution (50 mg/ml in 10 mM HEPES) was added to the medium.

CV1 Cells CV1 cells were obtained from the ATCC. They were cultured in 10-cm Petri dishes at 5 % CO_2 and 37 °C in D-MEM supplemented with 10 % FCS and Glutamax.

Microscopy Cells used for microscopy were grown on 18 mm coverslips in their native medium. The native medium of CV1 cells was replaced with CO_2-independent medium prior to the experiments. For imaging, the coverslips were mounted in the imaging chamber a custom-built ring. For microscoping HeLa and HeLa Cav1-mRFP cells, this chamber was filled with the medium in which the cells were grown during the preceding night. For CV1 cells the imaging chamber was filled with 1 ml CO_2-independent medium. All imaging was performed at 37 °C.

2.4.2 Transfection

To introduce plasmid DNA into HeLa and HeLa Cav1-mRFP cells they were transfected with the Nucleofactor Kit R (Amaxa). CV1 cells were transfected with the Nucleofac-

tor Kit V (Amaxa). Cells of a nearly confluent 10 cm dish were first washed and then trypsinized with 2 ml trypsin solution for several minutes. Then 8 ml of the native cell culture medium were added to the trypsinized cells. The cells were singularized by pipetting and an aliquot of 1.5 ml of this cell solution was then centrifuged in an Eppendorf tube for 10 min at 210 × g. Meanwhile a 12-well plate was prepared with a coverslip and 1 ml of the native cell culture medium each in four wells. Also an additional Eppendorf tube was filled with 0.5 ml medium. After centrifugation, the supernatant was removed and the cells were resuspended in 100 μl Nucleofactor Solution R for HeLa and HeLa Cav1-mRFP cells and 100 μl Nucleofactor Solution V for CV1 cells respectively. 2 μg DNA were added and the whole solution was transfered to an electroporation cuvette. HeLa and HeLa Cav1-mRFP cells were electroporated with program I-13. For CV1 cells the program A-24 was used. Immediatly after electroporation the cells were transfered to the prepared Eppendorf tube with 0.5 ml medium. Then they were equally distributed to the four coverslips in the 12-well plate and incubated overnight.

2.4.3 TIRF Microscopy

For TIRF microscopy, transfected cells on a 18 mm coverslip were mounted in the imaging chamber and covered with medium as mentioned before. The chamber was put onto the stage of the microscope, which was surrounded by a heated (37 °C) acrylic glass chamber. TIRF microscopy was performed with the Olympus 60× objective. The microscope allowed both epifluorescence and through-the-objective evanescent field illumination. Emitted light was collected with a CCD camera. The total internal reflection angle was manually adjusted for every experiment.

Fluorophores were excited by the evanescent field caused by a laser beam of the Kr-Ar laser introduced through the objective. For epifluorescence illumination of the fluorescent molecules light from a monochromator was used. The same wavelengths were used for TIRF and epifluorescence microscopy. Green fluorescent protein (GFP) and monomeric red fluorescent protein (mRFP) constructs were excited with light of 488 nm and 568 nm wavelength respectively. Yellow fluorescent protein (YFP) was also excited at 488 nm, Alexa Fluor 647 at 647 nm. For single and dual color experiments with the fluorophores GFP, enhanced GFP (EGFP), mRFP and YFP a dichroic mirror was used that allowed excitation with light of 488 and 568 nm wavelength and collection of the light emitted by these constructs. Another dichroic mirror that enabled excitation with light of 488, 568 and 647 nm wavelength and collection of the emission light of EGFP, mRFP and Alexa Fluor 647 (AF647) was used for triple-color experiments.

Imaging was done with the TILLvisION 4.0 software. Videos were made with a frame rate of 0.5 Hz. To gain higher temporal resolution frame rates of 4 Hz and 10 Hz were used as indicated. To image the single frames of 0.5 Hz movies, the fluorophores were excited sequentially either through evanescent illumination for 200 ms or epifluorescence illumination for 300 ms. To record movies of higher frame rates the exposure time and visible area had to be reduced. Single cells were imaged for up to 600 s, cells on one coverslip for a maximum of 2 h.

After the experiment, the cells that had been recorded were imaged by differential interference contrast microscopy to check the cells for viability.

2.4.4 Cholera Toxin Uptake

The internalization studies were performed using a recombinant cholera toxin subunit B (here refered to as choler toxin B) coupled to AF647. Transfected cells were cultured overnight on coverslips in their native medium in a 12 well plate. All media and solutions were prewarmed to 37 °C prior to use. Before the experiments, the medium was replaced by 1 ml CO_2-independent medium. A coverslip was taken out of the 12 well plate and 100 μl of cholera toxin B-AF647 (1 mg/ml) diluted 1:1000 with CO_2-independent medium was added. After 1 min incubation the cholera toxin B-AF647 solution was removed and the coverslip washed by dipping into CO_2-independent medium. The coverslip was mounted in the imaging chamber and covered with 1 ml CO_2-independent medium and immediatly imaged. One coverslip was imaged for a maximum of 30 min.

2.4.5 Image Processing and Data Analysis

Greyscale videos taken with the TILLvisION software were automatically intensity scaled and then exported as single tiff files which included all frames. For analysis of the videos, they were opened with ImageJ. Further analysis was performed as described in the results section.

3 Results

3.1 Time Resolution of Caveolar Endocytosis

3.1.1 Imaging of Caveolae by TIRF Microscopy

Individual caveolae can be visualized in live cells by expressing their major component caveolin 1 coupled to a fluorescent protein as EGFP or mRFP without disturbing their function [21]. By the use of TIRF microscopy, it has been made possible to resolve the internalization of caveolae labeled with caveolin 1-EGFP [22]. Caveolae that move away from the coverslip-proximal plasma membrane of cells leave the evanescent field and thereby lose detectable fluorescence signal. Such events can thus be identified as internalization because the decay in fluorescence intensity is faster than in the case of photobleaching.

Live HeLa Cav1-mRFP cells were imaged in TIRF mode. Since the phosphatase inhibitor orthovanadate (Na_3VO_4) enhances caveolar uptake of simian virus 40 (SV40) [13] we stimulated internalization of caveolae by incubating the cells with 1 mM orthovanadate. Caveolin 1-mRFP was excited by the 568 nm laser line in TIR illumination for 200 ms. As an image rate of 0.5 Hz yielded good results to visualizing clathrin-mediated endocytosis [5] we imaged the cells with the same frequency.

To qualitatively evaluate the recorded image series, images were automaticly intensity scaled and exported as a single multi-page 16 bit tiff file from the TILLvisION software. For evaluation, movies were opened with ImageJ and searched for individual caveolin-mRFP spots fading faster than photobleaching. Quantification of fluorescent signal was performed using measure macros in ImageJ. Further image processing for presentation purposes was performed with ImageJ and Photoshop, to which single frames were transfered as 8 bit single layer tiff files.

When imaging HeLa Cav1-mRFP cells in TIRF mode, a punctate pattern of caveolin 1-mRFP is visible throughout the cell (Figure 2 b). In general, two different kinds of caveolin 1-mRFP spots could be distinguished. Smaller spots differing slightly in brightness and larger structures with a undefined shape which were brighter than the caveolae. Because of the diffraction limit the diameter of neither of these spots could be determined. As these smaller spots were clearly separated structures relatively homogeneous in intensity profile, they very likely represent individual caveolae and are thus termed caveolae. While the large structures were mainly immobile, the smaller spots, individual caveolae, exhibited at least three different behaviors. The first group encloses caveolae that are immobile or tumbling around within a small area, secondly some caveolae are tumbling around before they suddenly disappear. The remaining caveolae were highly active. They appeared, were highly mobile and dissappeared within seconds or minutes, often repeatedly. We concentrated our analysis on spots of the second and third category, that were likely to internalize. The amount of internalized caveolae differed from cell to cell. In some cells hardly any internalization events were observed, whereas in others so many events could be captured that a thorough quantification was impossible.

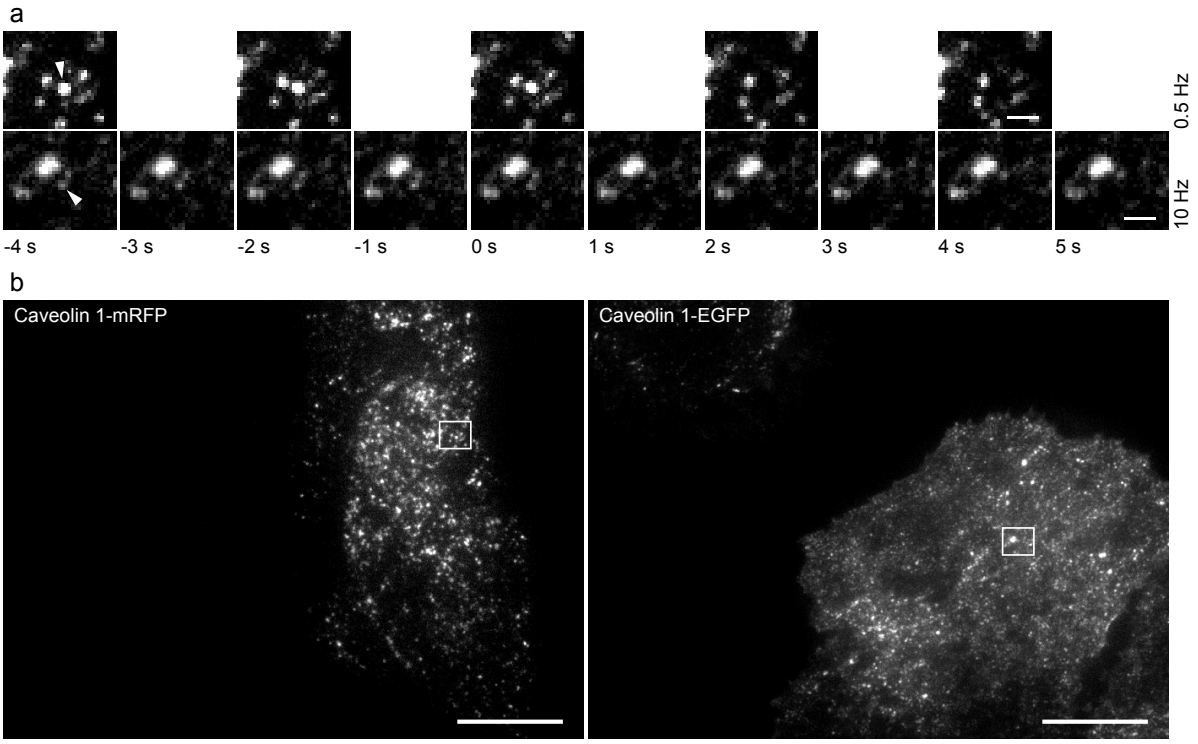

Figure 2: Internalization of caveolae observed by TIRF microscopy. (a) Time-series of caveolin 1-mRFP imaged at 0.5 Hz (top) and caveolin 1-EGFP recorded at 10 Hz (bottom). Times refer to the moment of departure defined in Figure 3. (b) Overview of the cells shown in (a). The left panel corresponds to the top series of (a), the right panel to the bottom one. Experiments were performed with HeLa Cav1-mRFP cells and HeLa cells transfected with caveolin 1-EGFP. Scale bars represent 0.8 μm (a) and 10 μm (b).

We did not find a correlation between the extent of caveolae internalization and the duration of orthovanadate stimulation.

We found that TIRF imaged caveolae vanished between two frames of time series recorded at 0.5 Hz (Figure 2 a), making it impossible to resolve the time resolution of caveolar endocytosis at this acquisition speed. To record movies with higher frame rates, the exposure time of the fluorophore had to be reduced. This however resulted in a insufficiently weak signal. Because of the much higher quantum yield of the fluorophore EGFP, we changed to a caveolin 1-EGFP fusion protein.

Videos of HeLa cells transfected with caveolin 1-EGFP were acquired now at a framerate of 10/s with 70 ms excitation by the 488 nm laser line in TIR mode. Because of limited memory and data transfer capacity of the camera the imaged area was reduced to a square of 200 pixels side length.

The pattern of the caveolin 1-EGFP fluorescence was indistinguishable from caveolin 1-mRFP fluorescence, only less of the large structures observed in HeLa Cav1-mRFP cells were present in the HeLa cells transfected with caveolin 1-EGFP. Like in HeLa Cav1-mRFP cells, caveolae exhibited the same three behaviors. We focused on caveolae that were suddenly dissappearing and on such that were visible only for a short time. The internalization of caveolae classified as the disappearance of a spot could be seen to occur within a timespan of several images (Figure 2 a), but some caveolae vanished within two subsequent frames. However, this happened only in a minor population.

We concluded that an imaging rate of 10 Hz is sufficient to resolve the internalization of fluorescently labeled caveolae.

3.1.2 Novel Tools for the Quantification of TIRF Microscopy Images

The quantification of the images required new computional tools. Despite a large variety of software available to qualitatively evaluate data in ImageJ, no existant tool satisfied the needs to quantify the acquired amount and complexity of data. Therefore, it was necessary to develop instruments to automatically follow and quantify fluorescence intensity of mobile caveolae in time lapse movies.

Finding Disappearing Spots Disappearing spots were identified by visual inspection of movies played and stopped by a custom made command for ImageJ. The mean fluorescence intensity from 3–5 pixel diameter circles circumventing individual disappearing caveolae was measured for every frame and the position noted.

Step Measure is a Plugin for Manual Tracking Since lateral movement during internalization required manual tracking, a new plugin was created. First, a macro was recorded, which adjusted the measurement settings, measured the mean intensity and current position of the region of interest (ROI) and finally switched to the next slide. The acquired data were exported a as text file. This macro was transformed to a plugin with the internal macro-to-plugin converter of ImageJ. The source code of the Step Measure plugin is shown in the appendix B.1. The plugin was compiled with the Java compiler embedded in ImageJ; it was accessed by the keybord shortcut “b”.

After every repeat of this plugin, measuring the mean intensity of the current ROI, the position was adjusted by the arrow keys and the plugin was run again. This plugin made it possible to manually track a caveolae through a whole image stack in a relatively short time.

The Plugin Tracer Follows Recorded Tracks To separate tracking and measurement, a novel plugin for ImageJ was written in Java to perform the tasks mentioned above. The source code of this plugin is shown in the appendix B.2. As the other plugin we compiled it with the internal compiler of ImageJ. This plugin was designed to read position data from the produced text file, measure mean fluorescence intensity in the respective ROI and optionally mark the ROI as measured in the movie. It has the capacity to measure the mean intensity of ROI in different channels of a movie. Due to its function to follow already recorded traces we called this plugin Tracer.

3.1.3 Internalization of Individual Caveolae

When screening for internalizing caveolae within the recorded 0.5 Hz movies of HeLa Cav1-mRFP cells and the 10 Hz movies of HeLa cells transfected with caveolin 1-EGFP, only spots present for at least a second were regarded.

Quantitative fluorescence data acquired with the help of the plugins were imported into Excel for further analysis. For averaging, all acquired traces were phase shifted to overlap in the moment of departure. The moment of departure of a caveolae was defined as the timepoint, when the first derivative of the intensity function reached its global minimum. The mean intensity values of traces from 0.5 Hz movies were then normalized by setting the mean of 10 consecutive mean intensity values of caveolae before departure from the plasma membrane to 1 and the minimum of the whole trace, which was basically background fluorescence, to 0. For 10 Hz movies, the mean of 20 consecutive data points was set to 1. All other values were intrapolated linearly (Figure 3 a and c). All acquired traces were then overlaid. The average of 20 traces from 0.5 Hz movies and of 29 traces of 10 Hz movies was calculated and plotted for visualization (Figure 3 b and d).

To determine the time constant of caveolae internalization we exported the average of the traces from the 10 Hz movies to Kaleidagraph. As the TIRF field declines exponentially [16, 17] we fitted an exponentional curve to the datapoints ranging from the time of departure at 0 s to 1.5 s post departure (Figure 4). As formula for the fitting we used $I = a + b \cdot \mathrm{e}^{-ct}$ where t were the times, I the corresponding intensity values, and a, b and c the parameters used for fitting. The time constant τ for the internalization of caveolae defined as the time required for the signal to drop to 1/e of its initial value was calculated with $\tau = 1/c$ and found to be 0.4 s. The half-life $t_{1/2}$ was 0.3 s.

We concluded, that an image rate of 10 Hz is sufficient to quantify the internalization of caveolae. Caveolae internalize form the plasma membrane with a half time of 0.3 s.

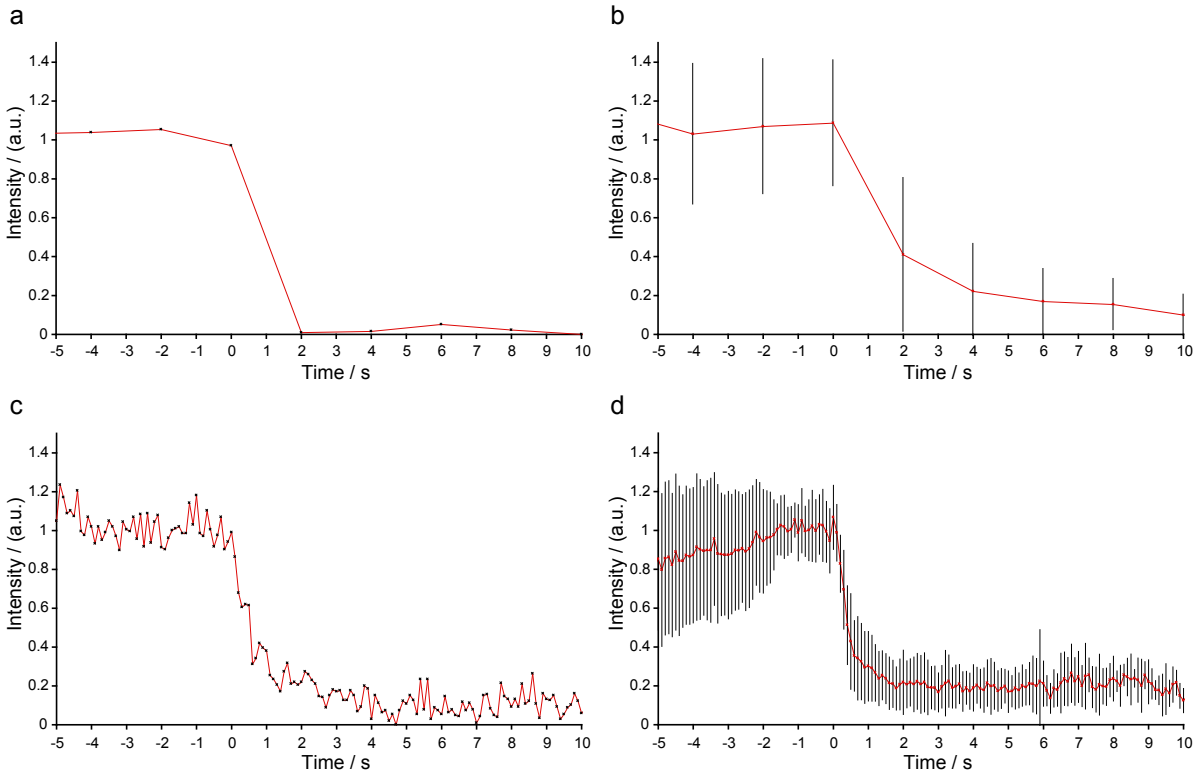

Figure 3: Time frame of caveolin internalization. (a and c) Fluorescence intensity of a caveolin internalization event recorded with 0.5 Hz (a) and 10 Hz (c) against time. (b) 20 traces as in (a) were phase shifted, normalized and averaged as described in the text. (d) Average of 29 phase shifted and normalized traces as in (c). The error bars in (b) and (d) represent the standard deviation. Traces in (a) and (b) are from HeLa Cav1-mRFP cells; traces in (c) and (d) from HeLa cells transfected with caveolin 1-EGFP.

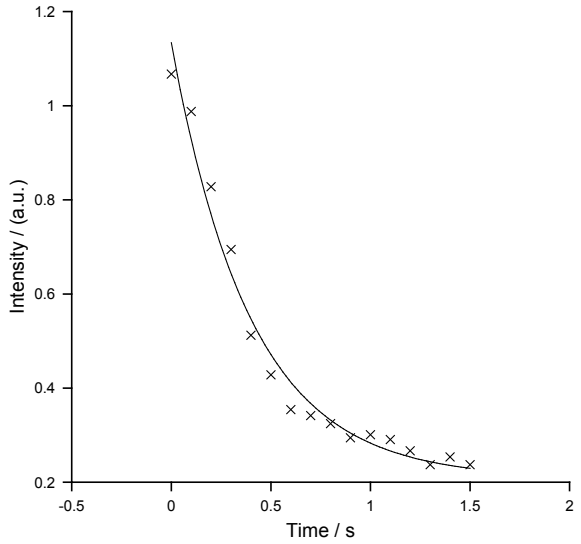

Figure 4: The average fluorescence intensity trace of internalizing caveolae can be fitted exponentially. The normalized and averaged fluorescence intensity values of traces from 10 Hz movies (Figure 3 d) were fitted with Kaleidagraph. As formula $I = a + b \cdot \mathrm{e}^{-ct}$ was used. The time constant τ was 0.4 s, the half-life $t_{1/2} = 0.3$ s.

3.2 Caveolae and the Actin-Based Endocytic Machinery

3.2.1 Caveolae and Actin

It was shown previously, that actin is involved in several endocytic pathways. Extensive studies by TIRF microscopy visualized the recruitment of actin to clathrin-coated pits [4, 5, 6]. Several different experiments implicate an important role of the actin-based machinery in caveolar endocytosis. However, the recruitment of actin to caveolae was not studied by TIRF microscopy so far.

To investigate the role of actin in caveolar endocytosis, we transfeced HeLa Cav1-mRFP cells with EGFP-actin. Caveolar endocytosis was stimulated by incubating the cells with 1 mM orthovanadate. To get an overview of the extent of the relationship of EGFP-actin and caveolin 1-mRFP we recorded 0.5 Hz dual-color TIRF movies. Single frames were acquired sequentially by exciting first caveolin 1-mRFP and then EGFP-actin for 200 ms in TIRF mode.

Under TIRF illumination of EGFP-actin, actin stress fibres were most prominent. In between the stress fibres, small spots and worm like struktures were apparent, while waves of reorganizing actin were seen at the edges of the cells (Figure 5 b). Since a diffuse distribution of monomeric actin between the stress fibres made it impossible to distinguish specific actin aggregates, cells with a low expression level of EGFP-actin were chosen for microscopy.

The movies were analyzed with ImageJ by merging the caveolin 1-mRFP to the red channel and EGFP-actin to the green channel of an RGB movie. We adjusted

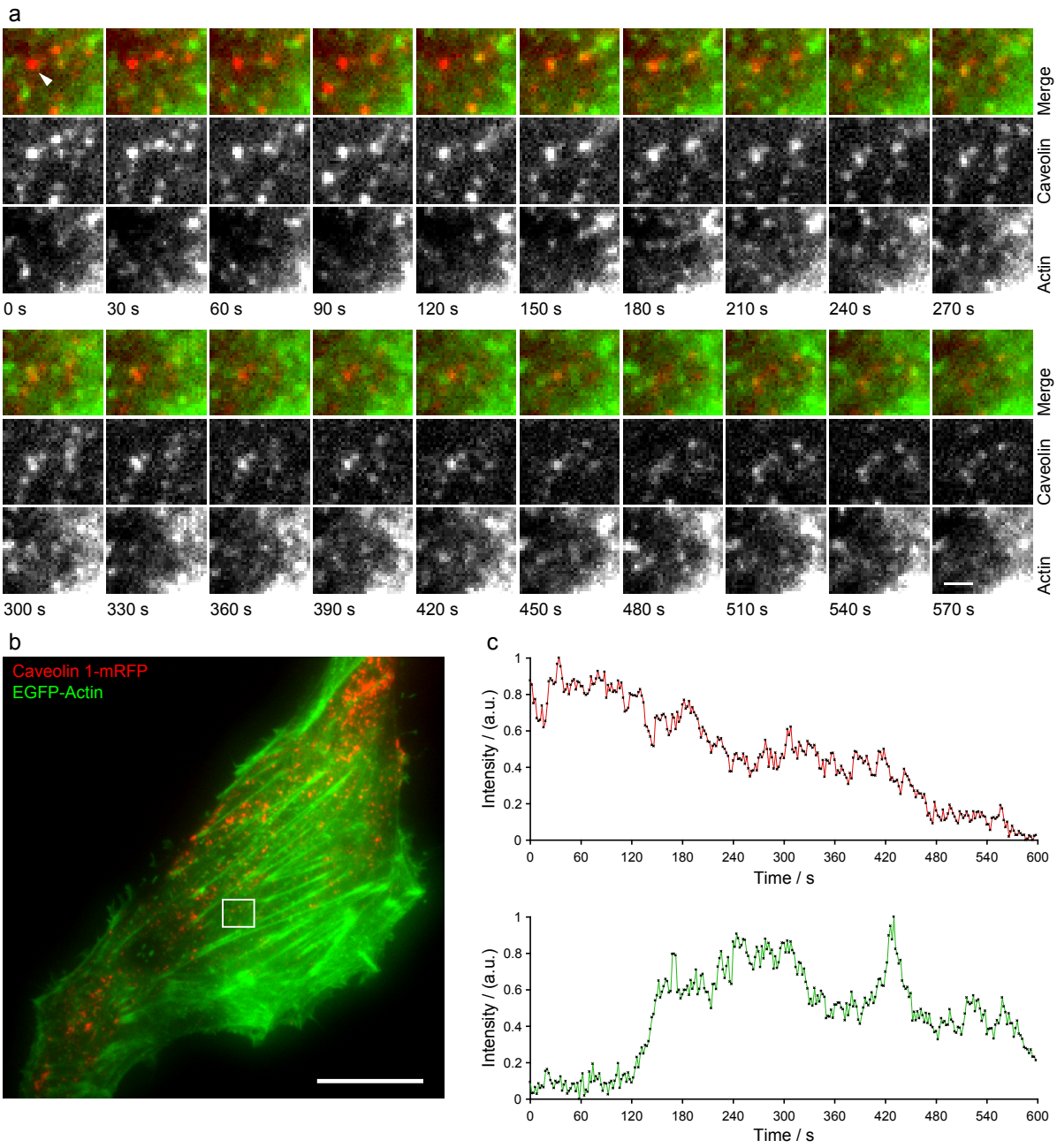

Figure 5: Actin recruitment to caveolae. (a) Images of a caveola (middle) and actin fluorescence (bottom). The top row shows the merged images. EGFP-actin is recruited to a spot of caveolin 1-mRFP. (b) Overview of the merged images. (c) Fluorescence intensity of caveolin 1-mRFP (top panel) and EGFP-actin (lower panel) plotted against time. The caveola was tracked manually and the EGFP-actin fluorescence intensity followed by automatic tracing the same track. The measured signal was normalized. HeLa Cav1-mRFP cells were transfected with EGFP-actin, stimulated with 1 mM orthovanadate and visualized by TIRF microscopy. Scale bars represent 0.8 μm (a) and 10 μm (b).

the levels for the single channels and screened the merged movies for yellow areas, which indicate the presence of both EGFP-actin and caveolin 1-mRFP. We detected some caveolae colocalizing with the actin stress fibres (Figure 5 b). However, these caveolae were immobile and did not internalize. Occasionally, we found individual caveolin spots which had colocalizing actin spots (Figure 5 a). At some of these caveolae, EGFP-actin fluorescence increased. We manually tracked such caveolae with the help of the Step Measure plugin. The recorded traces were then used to follow the recruitment of actin in the EGFP-actin fluorescence channel with the Tracer plugin. The recorded traces were normalized by setting the maximum mean intensity value to 1 and the minimum to 0. All other values were intrapolated linearly (Figure 5 c).

Although EGFP-actin is clearly recruited to some internalizing caveolae, not all internalizing caveolae show transient actin recruitment. We can not conclude to a general requirement of actin for caveolar endocytosis from our data.

3.2.2 Caveolae and Arp3

The high background of monomeric EGFP-actin fluorescence in the cytoplasm could obstruct visualization of transient actin polymerization at internalizing caveolae. Actin polymerization requires the actin nucleating Arp2/3 complex, which consist of seven different proteins. Since the Arp2/3 complex component Arp3 coupled to GFP gives clearly resolved staining in individual spots, we assumed that this marker would be more suited to visualize local actin polymerization events. To investigate actin nucleation induced by the Arp2/3 complex during cavoelar endocytosis, we transfected HeLa Cav1-mRFP cells with Arp3-EGFP. We incubated the cells with 1 mM orthovanadate and analyzed them by TIRF microscopy. We recorded 0.5 Hz dual-color TIRF movies.

A diffuse distribution of Arp3-EGFP was observed throughout the whole cell. Only few spots of Arp3-EGFP were visible (Figure 6). We screened for colocalization by merging the Arp3-EGFP channel and the caveolin 1-mRFP channel. Only few colocalization events were found. Unexpectedly, the caveolae with colocalizing Arp3-EGFP staining tumbled around at the plasma membrane and did not internalize (Figure 6).

We concluded, that Arp3 can be recruited to caveolae, however the resulting signal was not sufficient to make quantitative statements.

3.2.3 Caveolae and Cortactin

Cortactin is a F-actin binding protein that can interact with several other proteins of the actin cytoskeleton. It was shown, that cortactin is required for clathrin-mediated endocytosis [7] as well as for the clathrin-independent internalization of the γc cytokine receptor [23], but so far the relationship between coveolin dependent endocytosis and cortactin has not been explored.

To examine the role of cortactin during caveolar endocytosis, we used HeLa Cav1-mRFP cells transfected with cortactin-EGFP. The cells were visualized by TIRF microscopy by recording dual-color TIRF movies with a frame rate of 0.5 Hz. The movies were examined with ImageJ as described before.

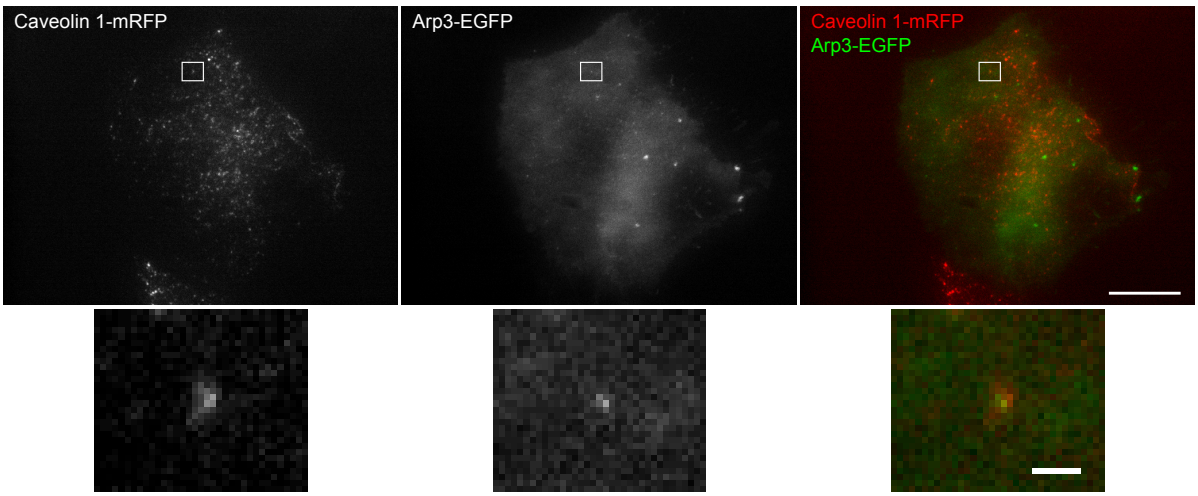

Figure 6: Arp3 colocalizes with caveolae. The lower panels show an enlargement of the boxes in the top panels. HeLa Cav1-mRFP cells were transfected with Arp3-EGFP, stimulated with 1 mM orthovanadate and visualized by TIRF microscopy. Scale bars represent 10 μm and 0.8 μm (enlargement).

Cortactin-EGFP showed an distinct pattern when observed by TIRF microscopy. Cortactin-EGFP is localized to spots at or near the plasma membrane distributed over the whole cell surface. It is accumulated at the edges of the cell in filopodia and lamellipodia. By screening the movies, we found several colocalization-events of caveolae with cortactin-EGFP (Figure 7).

Since we found several colocalization-events between caveolin 1-mRFP and cortactin-EGFP, we decided to investigate this relationship further. Because 10 Hz movies would have resulted in small excitation times leading to fluorescence intensities to low for conclusive data, we recorded movies at 4 Hz. HeLa Cav1-mRFP cells were transfected with cortactin-EGFP. Cells were incubated with 1 mM orthovanadate and visualized by TIRF microscopy. Caveolin 1-mRFP was excited with the 568 nm laser line for 100 ms and subsequently cortactin-EGFP was excited with the 488 nm laser line for 93 ms. Cells were imaged for 250 s. Movies were analyzed using ImageJ as described before.

Caveolae colocalizing with diffuse cortactin-EGFP staining could be observed. Most of these caveolae were tumbling around with the cortactin staining following the movement. Also disappearing caveolin spots were found. However cortactin-EGFP was not found to accumulate additionally at the vanishing spot. Nevertheless, the cortactin-EGFP staining disappeared mostly shortly after the colocalizing caveolae (Figure 8 a).

To quantify the comigration of cortactin-EGFP and caveolin 1-mRFP staining, we manually tracked the caveolae with the Step Measure plugin for ImageJ. The recorded traces were then used to follow the fluorescence intensity of cortactin-EGFP with the Tracer plugin. The recorded traces were normalized by setting the maximum mean intensity value to 1 and the minimum to 0. All other values were intrapolated linearly (Figure 8 c). We found that some caveolae exhibited synchronous intensity fluctuations

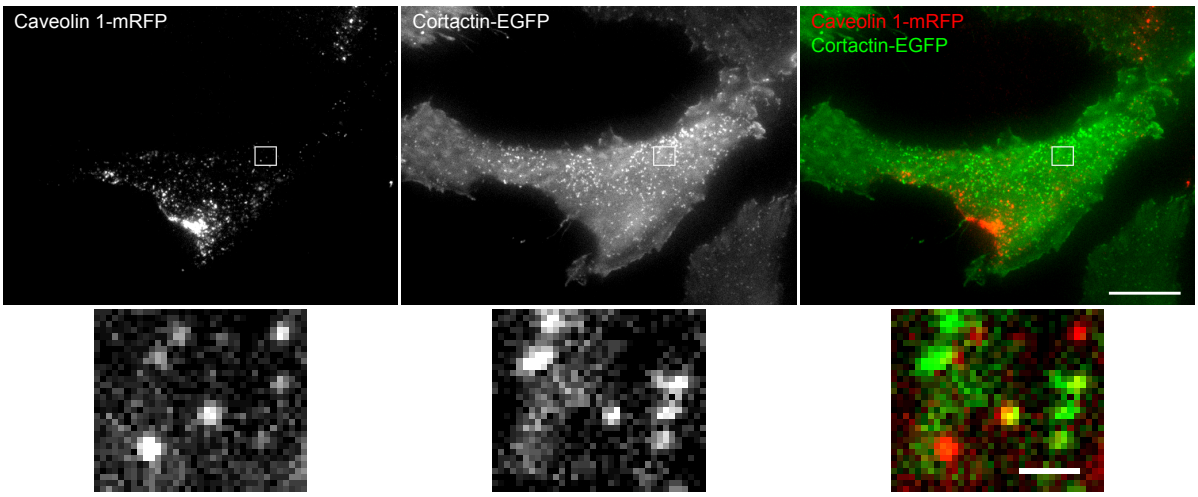

Figure 7: Cortactin colocalizing with caveolae. The lower panels show an enlargement of the boxes in the top panels. HeLa Cav1-mRFP cells were transfected with cortactin-EGFP and visualized by TIRF microscopy. Scale bars represent 10 μm and 0.8 μm (enlargement).

in the caveolin 1-mRFP channel and the cortactin-EGFP channel. Local maxima in the caveolin channel coincided with local maxima in the cortactin channel (Figure 8 c). However, other caveolae showed a contradictory behaviour. The fluorescence intensity in the cortactin-EGFP channel fluctuated alternating with that of the caveolin 1-mRFP channel. In this case, local minima in the cortactin-EGFP channel were observed at local maxima in the caveolin 1-mRFP channel and vice versa.

These different behaviors may reflect different spatial positions of cortacin-EGFP to caveolae in the evanescent field, during the previously described kiss and run cycling of caveolae through the actin cortex [24].

3.3 Signaling Involved in Caveolar Endocytosis

The internalization of caveolae is a triggered process [13, 25], that involves phosphorylation induced by ligand addition. However, little is known about the complex arrangement of the triggering process. It may occur through clustering of lipid raft components as for example glycosylphosophatidylinositol (GPI)-anchored proteins or gangliosides by the addition of multimeric ligands. This clustering is thought to result in recruitment of cytosolic or transmembrane signaling factors such as tyrosine kinases and their substrates. The resulting signaling casacade ends in endocytic internalization.

3.3.1 Caveolae and Dynamin

Dynamin is a GTPase that is required for fission and internalization in clathrin-mediated endocytosis as well as in caveolar endocytosis [26, 27]. It localizes to the neck of cave-

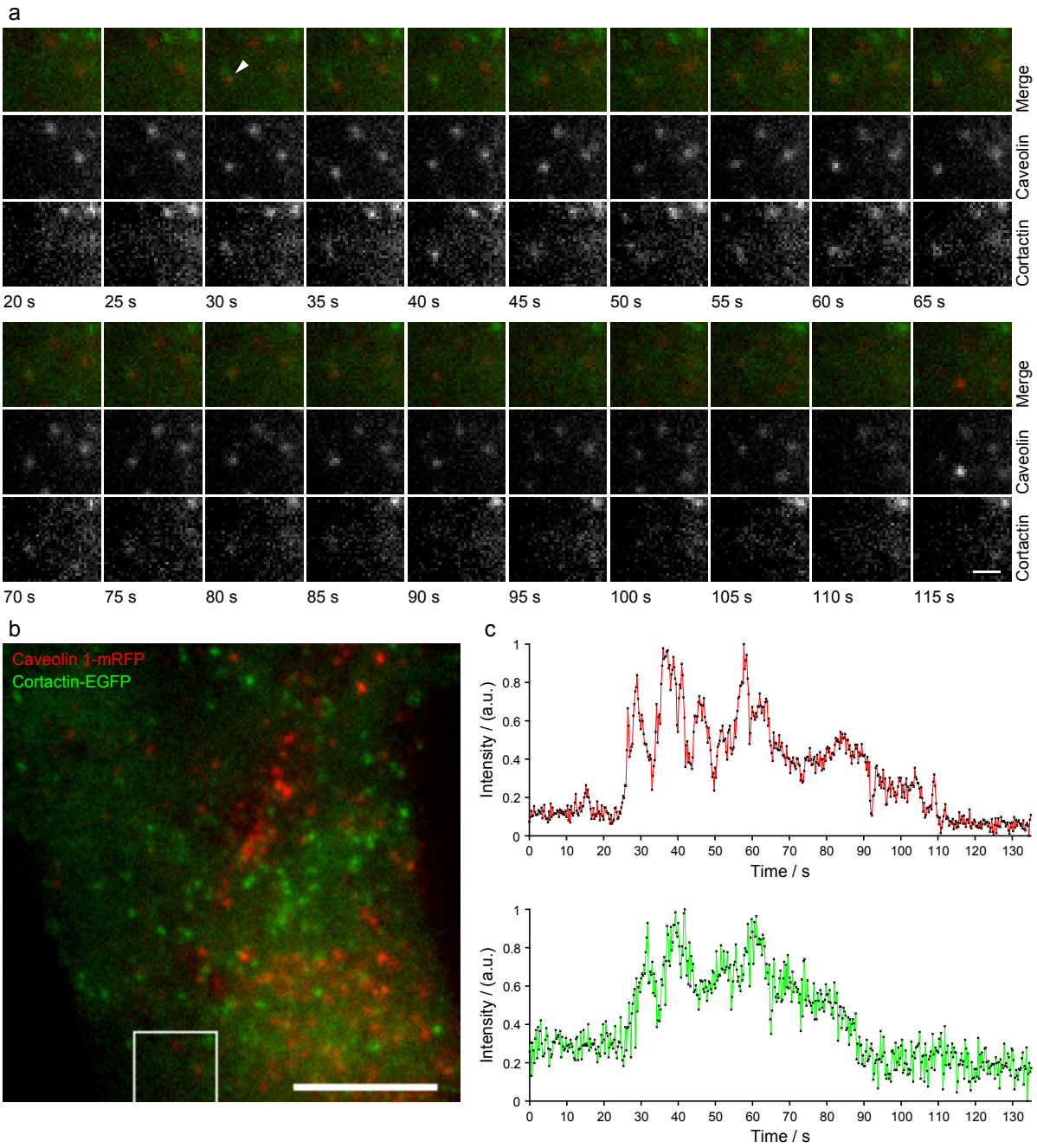

Figure 8: Cortactin colocalizes with caveolae. (a) Images of a caveola (middle) and cortactin fluorescence (bottom). The top row shows the merged images. Diffuse cortactin-EGFP staining is associated with an appearing and disappearing caveola. (b) Overview of the merged images. (c) Fluorescence intensity of caveolin 1-mRFP (top panel) and cortactin-EGFP (lower panel) plotted against time. The caveola was tracked manually and the cortactin-EGFP fluorescence intensity followed by automatic tracing of the same track. The measured signal was normalized. HeLa Cav1-mRFP cells were transfected with cortactin-EGFP, stimulated with 1 mM orthovanadate and visualized by TIRF microscopy. Scale bars represent 0.8 μm (a) and 10 μm (b).

olae. Recently, a direct interaction of caveolin 1 with dynamin 2 was found in *in vitro* studies [28]. Because of its multiple interaction partners and binding sites, it is likely that dynamin 2 acts as an scaffold protein in signaling required for caveolar endocytosis.

To visualize the interaction of dynamin with caveolin by TIRF microscopy, we double-transfected CV1 cells with both caveolin 1-mRFP and dynamin 2-EGFP. We used CV1 cells, because we speculated to trigger caveolar endocytosis with SV40. CV1 cells originate from african green monkey, the natural host of SV40. We acquired dual-color TIRF movies with a frame rate of 0.5 Hz and analyzed the movies using ImageJ.

The pattern of caveolin 1-mRFP staining in CV1 cells shows differences to that in HeLa Cav-mRFP cells. On the bottom surface, when imaged in TIRF microscopy, several dark stripes lacking caveolin 1-mRFP fluorescence were visible. The caveolin spots in between these stripes were more densely scattered than in HeLa cells. The caveolae spots also seemed larger (Figure 9 c).

We screened for colocalization of dynamin 2-EGFP with caveolin 1-mRFP using ImageJ as described above, and found immobile caveolae with associated dynamin 2-EGFP, but only very few caveolae exhibited dynamin 2 staining. However, often it was not clearly distinguishable, whether these events were in fact colocalization or just nearby individual dynamin 2-EGFP and caveolin 1-mRFP spots.

Appearing and disappearing caveolin 1-mRFP spots that recruit dynamin 2-EGFP were also found (Figure 9 a). Also, slowly laterally moving caveolae with associated diffuse dynamin 2-EGFP staining were detected (Figure 9 b).

From these observations we conclude that dynamin 2-EGFP can localize to appearing and vanishing caveolae as well as to mobile ones.

3.3.2 Phosphorylation

One of the most common signaling mechanisms is phosphorylation. In eukaryotes most cellular phosphorylation occurs on serine and threonine residues. But phosphorylation of tyrosine residues is essential for the regulation of many cellular processes. Caveolin 1 is phosphorylated on tyrosine residue 14 in response to stimuli or when the cells are exposed to oxidative stress.

YFP-dSH2 Src family kinases are involved in the phosphorylation of caveolin 1. The Src homology 2 (SH2) domain binds to phosphorylated tyrosine residues.

To examine temporal phosphorylation during caveolar endocytosis, we double-transfected CV1 cells with caveolin 1-mRFP and a YFP coupled to two consecutive SH2 domains (YFP-dSH2). We used a construct with two SH2 domains, because SH2-interactions with target proteins are relatively weak. The addition of a second SH2 domain recruits this construct to highly phosphorylated regions of the plasma membrane. Cells were imaged by TIRF microscopy by recording dual-color TIRF movies with a frame rate of 0.5 Hz. The movies were analyzed with ImageJ.

When observed by TIRF microscopy, YFP-dSH2 predominantly localized to focal adhesions (Figure 10 b). The fluorescence signal of YFP-dSH2 at these focal adhesions was so strong, that it rendered other YFP-dSH2 hardly detectable. An increase in

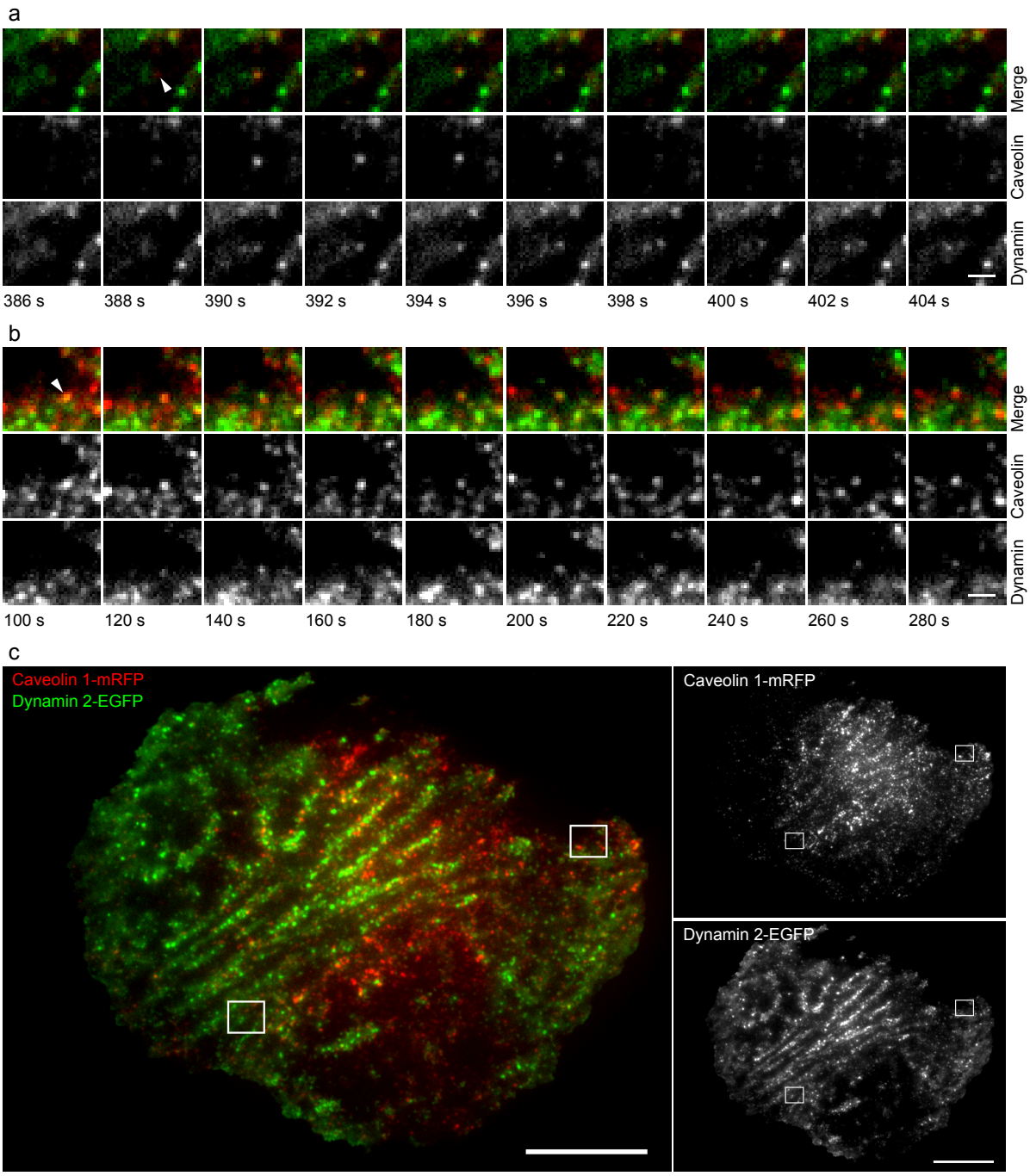

Figure 9: Dynamin colocalizes with caveolae. (a) and (b) Images of caveolae (middle) and dynamin fluorescence (bottom). The top row shows the merged images. Two different events are shown. Times refer to the overview shown in (c). (a) Dynamin 2-EGFP is recruited to an appearing and disappearing caveola. (b) Dynamin 2-EGFP colocalizes with a moving spot of caveolin 1-mRFP. (c) Overview of cell imaged in (a) and (b). The left box corresponds to (a) the right one to (b). The right panels show the single channels of the merged image in the left panel. CV1 cells were double-transfected with caveolin 1-mRFP and dynamin 2-EGFP, and visualized by TIRF microscopy. Scale bars represent 0.8 μm (a), (b) and 10 μm (c).

the level of the YFP-dSH2 signal made single spots detectable. These spots exhibited different behaviors. Some were laterally moving, while others were immobile.

Some YFP-dSH2 positive spots colocalized with immobile caveolae. However, most YFP-dSH2 spots were associated with fast laterally moving caveolae (Figure 10 a). We could further observe that caveolae were concentrated around the focal adhesions visualized by YFP-dSH2.

To examine the effect of increased phosphorylation associated with caveolae, we inhibited tyrosine phosphatases with orthovanadate. CV1 cells double-transfected with caveolin 1-mRFP and YFP-dSH2 were stimulated with 1 mM orthovanadate and imaged by TIRF microscopy. We acquired dual-color TIRF movies with an image rate of 0.5 Hz.

When analysing the movies with ImageJ, we could not find any differences between stimulated and unstimulated cells. As for unstimulated cells, we could observe a maximum of approximately four colocalization events per cell and 10 min. We also tried to qualitatively compare the mobility of caveolae in stimulated and unstimulated cells. We could neither establish any usefull algorithm to perform this task, nor find any differences. In general, the differences within the group of stimulated and unstimulated cells itself were larger than inbetween these two groups.

GFP-Grb2 Since the YFP-dSH2 construct showed less colocalization with caveolae than expected, we decided to investigate a naturally occuring phosphotyrosine binding protein. Growth factor receptor bound protein 2 (Grb2) is an adapter protein that has a SH2 domain sandwiched by two SH3 domains. Grb2 can itself be phosphorylated on a tyrosine residue at the C-terminus. It was shown to interact with various other proteins including such responsible for actin nucleation.

We analyzed the interaction of Grb2 with caveolin 1 by cotransfecting GFP-Grb2 and caveolin 1-mRFP into CV1 cells. We visualized the cells by TIRF microscopy by recording 0.5 Hz dual-color movies.

The pattern of GFP-Grb2 did not show a clearly defined distribution as YFP-dSH2. In general the signal was much more diffuse. Large stripes of GFP-Grb2 were visible. GFP-Grb2 also localized to adhesion contacts at the cell edges. In addition we observed diffuse spots (Figure 11 b).

When comparing the caveolin 1-mRFP signal with the GFP-Grb2 signal, we noticed that nearly no caveolae were located at places with very dense GFP-Grb2 staining. However, caveolae preferentially localized close to dense GFP-Grb2 staining.

When looking at the merged movies of the caveolin 1-mRFP channel and GFP-Grb2 channel, we found areas in which GFP-Grb2 staining colocalized with caveolin-1-mRFP signal. Colocalizing areas were very near the GFP-Grb2 stripes and no specific accumulation of GFP-Grb2 spots were visible. Also few single immobile or slowly moving caveolae with an associated cloud of GFP-Grb2 were detected (Figure 11 a).

As a conclusion we can say, that although it is a rarely observed event, caveolae do recruit GFP-Grb2.

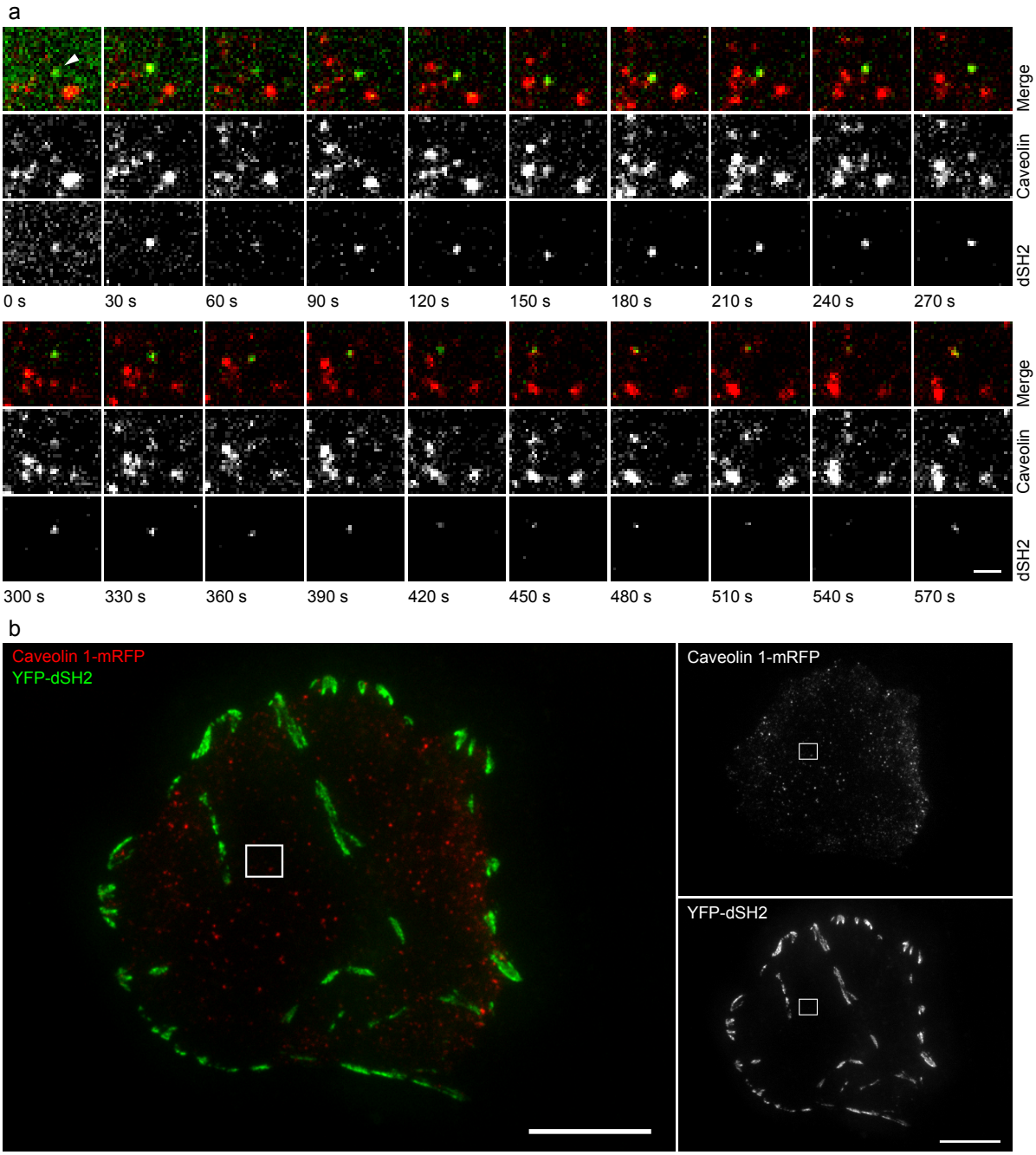

Figure 10: Tyrosine phosphorylation in caveolae. (a) Images of a caveola (middle) and YFP-dSH2 fluorescence (bottom). The top row shows the merged images. YFP-dSH2 colocalizes with a moving caveola. (b) Overview of the cell imaged in (a). The right panels show the single channels of the merged image in the left panel. CV1 cells were transfected with both caveolin 1-mRFP and YFP-dSH2, and imaged by TIRF microscopy. Scale bars represent 0.8 μm (a) and 10 μm (b).

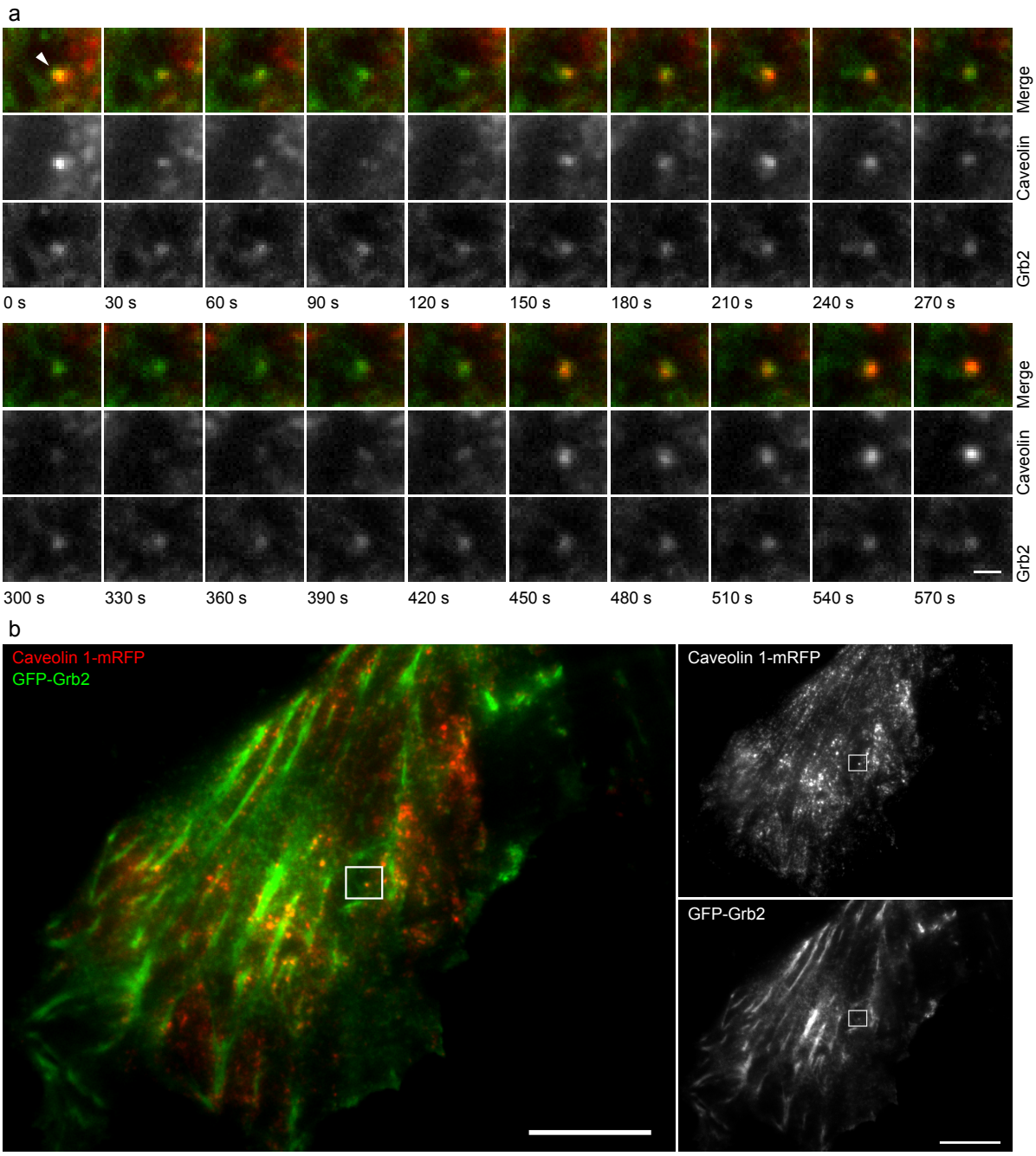

Figure 11: The adaptor protein Grb2 colocalizes with individual caveolae. (a) Images of a caveola (middle) and GFP-Grb2 fluorescence (bottom). The top row shows the merged images. GFP-Grb2, which binds through its SH2 domain to phosphorylated proteins, colocalizes with a stationary caveola. (b) Overview of the cell imaged in (a). The right panels show the single channels of the merged image in the left panel. CV1 cells were double-transfected with caveolin 1-mRFP and GFP-Grb2, and imaged by TIRF microscopy. Scale bars represent 0.8 μm (a) and 10 μm (b).

3.3.3 Phosphatidylinositol-4,5-bisphosphate

Phosphatidylinositols are lipids, that can act as signaling molecules in the inner leaflet of the plasma membrane. Dozens of proteins contain a domain first found in pleckstrin, that binds polyphosphoinositols. The pleckstrin homology (PH) domains of dynamin and phospholipase C-δ prefer phosphatidylinositol-4,5-bisphosphate (PIP_2) whereas the PH domains of other proteins may favor different phosphatidylinositols.

Since caveolae are enriched in PIP_2 [29, 30], we wanted to further investigate the role of this signaling mechanism in caveolar endocytosis. We double-transfected CV1 cells with both caveolin 1-mRFP and with the PH domain of phospholipase C-δ1 coupled to EGFP (PH-PLC-EGFP). Cells were analyzed by recording 0.5 Hz dual-color TIRF movies and examination of the movies with ImageJ.

Under TIR illumination, PH-PLC-EGFP is visible at the edges of the cells and in form of stripes at the bottom surface. Furthermore, small spots of the same size as individual caveolae were apparent. These spots were very dynamic. They moved laterally, appeared and disappeared. We analyzed this punctated pattern of PH-PLC-EGFP for colocalization with caveolin 1-mRFP staining, and found multiple such events (Figure 12). We screened for and found caveolae positive for PH-PLC-GFP staining, that appear, stay for some time, and disappear again (Figure 13 a). We manually tracked such spots with the Step Measure plugin for ImageJ in the caveolin 1-mRFP channel and traced them in the PH-PLC-EGFP channel with the Tracer plugin. The traces of the fluorescence intensity of both channels showed that the caveolin 1-mRFP spot and the PH-PLC-EGFP spot showed up synchronously (Figure 13 c). No additional recruitment or a peak of PH-PLC-EGFP during caveolae internalization was detectable.

From these observations we conclude that PIP_2 might play a role in caveolin signaling, but this signaling might not be directly linked to the endocytic event.

3.4 Ligand-Mediated Endocytosis

3.4.1 Caveolar Internalization of Cholera Toxin

It has been proposed, that caveolar endocytosis is ligand-mediated in contrast to the classical, receptor-mediated endocytic pathways. Since observation of internalizing caveolae in steady state did not result in highly specific data on the different constructs, we decided to concentrate on caveolae involved in endocytosis of specific ligands added live. We decided to use cholera toxin B subunit, a ganglioside-binding pentameric protein, that uses caveolae for endocytosis to identify ligand-activated caveolae.

We transfected CV1 cells with caveolin 1-mRFP and PH-PLC-EGFP. Next day, immediately before microscopy, cholera toxin B-AF647 at a concentration of 1 μg/ml was bound to live cells for 1 min, and the cells were washed. We acquired videos in TIRF mode of both caveolin 1-mRFP and PH-PLC-EGFP, while cholera toxin B-AF647 was excited by epifluorescence illumination. The acquisition rate was 0.5 frames per second. By using both epi- and TIRF-illumination, cholera toxin B-AF647 positive caveolae could be followed during endocytic internalization. Movies were analyzed with ImageJ as before.

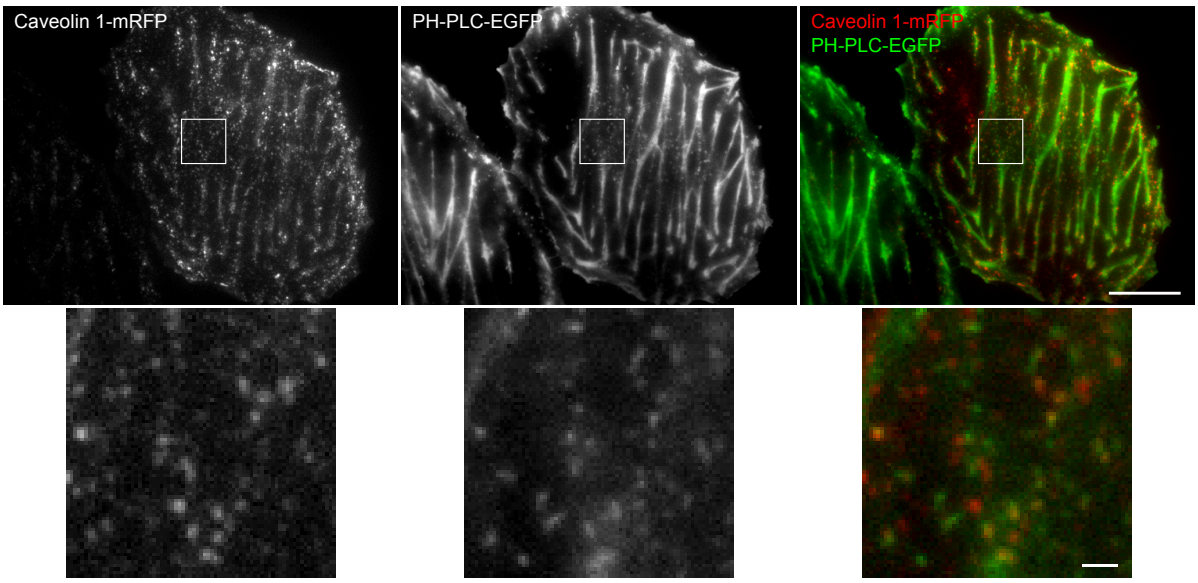

Figure 12: The PH domain of PLC-δ localizes to caveolae. The lower panels show an enlargement of the boxes in the top panels. Several spots of PH-PLC-EGFP, which binds to PIP_2, colocalize with caveolae. CV1 cells were double-transfected with caveolin 1-mRFP and PH-PLC-EGFP, and visualized by TIRF microscopy. Scale bars represent 10 μm and 0.8 μm (enlargement).

Comparison of the caveolin 1-mRFP TIRF channel with the cholera toxin B-AF647 epifluorescence channel revealed extensive colocalization on the cell surface (Figure 14 b). Within 10 minutes after binding, caveolae loaded with cholera toxin B-AF647 started to internalize. After 30 min cholera toxin B-AF647 accumulated to a large extent in the Golgi complex.

As expected, caveolin 1-mRFP spots disappeared by moving out of the evanescent field whereas cholera toxin B-AF647 signal remained visible under epifluorescence illumination (Figure 14 a). We manually tracked such events in the RGB movie containing the merged caveolin 1-mRFP and cholera toxin B-AF647 channels. Then we traced the fluorescence intensity in the single channels with the Tracer plugin for ImageJ. To correct for background, we measured the fluorescence intensity for both channels in a circular area for every frame used to track the internalization process. This area was of the same size as the area used for tracking. It also had to be within the cell and it was not allowed that an additional caveolin 1-mRFP or cholera toxin B-AF647 spot appeared in this area. The background values thus acquired were subtracted from the traced fluorescence intensity values of the caveolin 1-mRFP and cholera toxin B-AF647, respectively. Afterwards, the values were normalized independently for each channel. We observed events, in which the caveolin 1-mRFP signal from TIRF illumination dropped, while at the same time the intensity of epifluorescence excited cholera toxin B-AF647 remained constant for the same vesicle (Figure 14 c). We calculated the ratio of the background

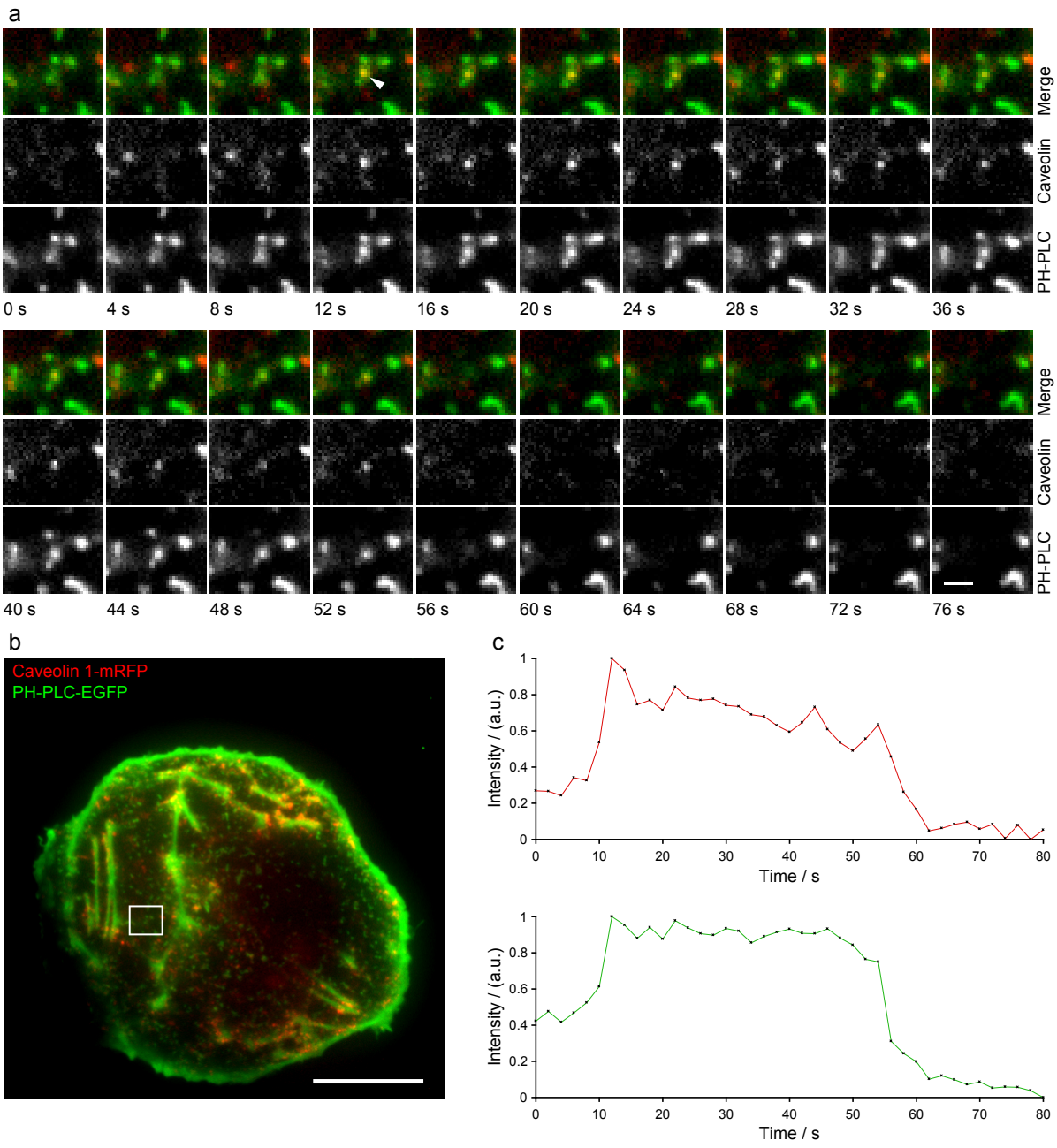

Figure 13: The PH domain of PLC-δ associates with caveolae. (a) Images of a caveola (middle) and PH-PLC-EGFP fluorescence (bottom). The top row shows the merged images. PH-PLC-EGFP appears and disappears simultanously with a spot of caveolin 1-mRFP. (b) Overview of the merged images. (c) Fluorescence intensity of caveolin 1-mRFP (top panel) and PH-PLC-EGFP (lower panel) plotted against time. The caveola was tracked manually and the PH-PLC-EGFP fluorescence intensity followed by automatic tracing the same track. The measured signal was normalized. CV1 cells were double-transfected with caveolin 1-mRFP and PH-PLC-EGFP, and imaged by TIRF microscopy. Scale bars represent 0.8 μm (a) and 10 μm (b).

corrected and normalized fluorescence intensity values of the trace of the cholera toxin B-AF647 epifluorescence movie and those of the trace of the caveolin 1-mRFP TIRF movie. A large increase in this ratio is observable as the caveolae internalize (Figure 14 d). Such events were scored as internalization events.

We were now able to observe and resolve individual ligand-mediated cointernalization-events and to quantify them.

3.4.2 Caveolar Endocytosis of Cholera Toxin and the PH domain

Since we found that the PIP_2 binding PH domain of PLC-δ accumulates in caveolae (Figure 12), we decided to examine the role of PIP_2 in caveolar uptake of cholera toxin.

For experiments we used the same CV1 cells transfected with caveolin 1-mRFP and PH-PLC-EGFP as for the cholera toxin B-AF647 internalization experiment. The cells were incubated with 100 μl cholera toxin B-AF647 solution (1 μg/ml), and videos were recorded with a frame rate of 0.5 Hz. In this case, cholera toxin B-AF647 and PH-PLC-GFP were excited by TIR illumination , while caveolin 1-mRFP was recorded in epifluorescence mode. The same image analysis as above was performed in ImageJ.

The overall PH-PLC-EGFP distribution seen by TIRF microscopy did not change upon cholera toxin addition (compare Figure 15 with 12 and 13 b). We found that both cholera toxin B-AF647 bound to the plasma membrane, or located in vesicles, did colocalize with caveolin 1-mRFP or PH-PLC-EGFP by merging the corresponding channels with the cholera toxin-AF647 channel. When merging all three channels to a RGB movie, few spots positive for all three markers were found. However, only three to five triple colocalization spots, that were stable for few seconds and comigrating, indicating enduring interaction, could be detected per cell during a time period of 10 min.

We found cholera toxin loaded caveolae which had associated PH-PLC-EGFP staining and stayed at the plasma membrane until they abruptly internalized. The spot of the internalizing caveolae also disappeared in the caveolin 1-mRFP epifluorescence channel by moving out of the focused area towards the center of the cell. Since the signal of PH-PLC-EGFP bleached rapidly, we were not able to analyze, whether the PH-PLC-EGFP staining was still associated with the caveolae, when it internalized (Figure 16).

We concluded from these observation that caveolae loaded with cholera toxin can be enriched in PIP_2. As many caveolae loaded with cholera toxin, but devoid of a PH-PLC-EGFP were detected, we cannot conclude to a requirement of PIP_2 for caveolar endocytosis of cholera toxin.

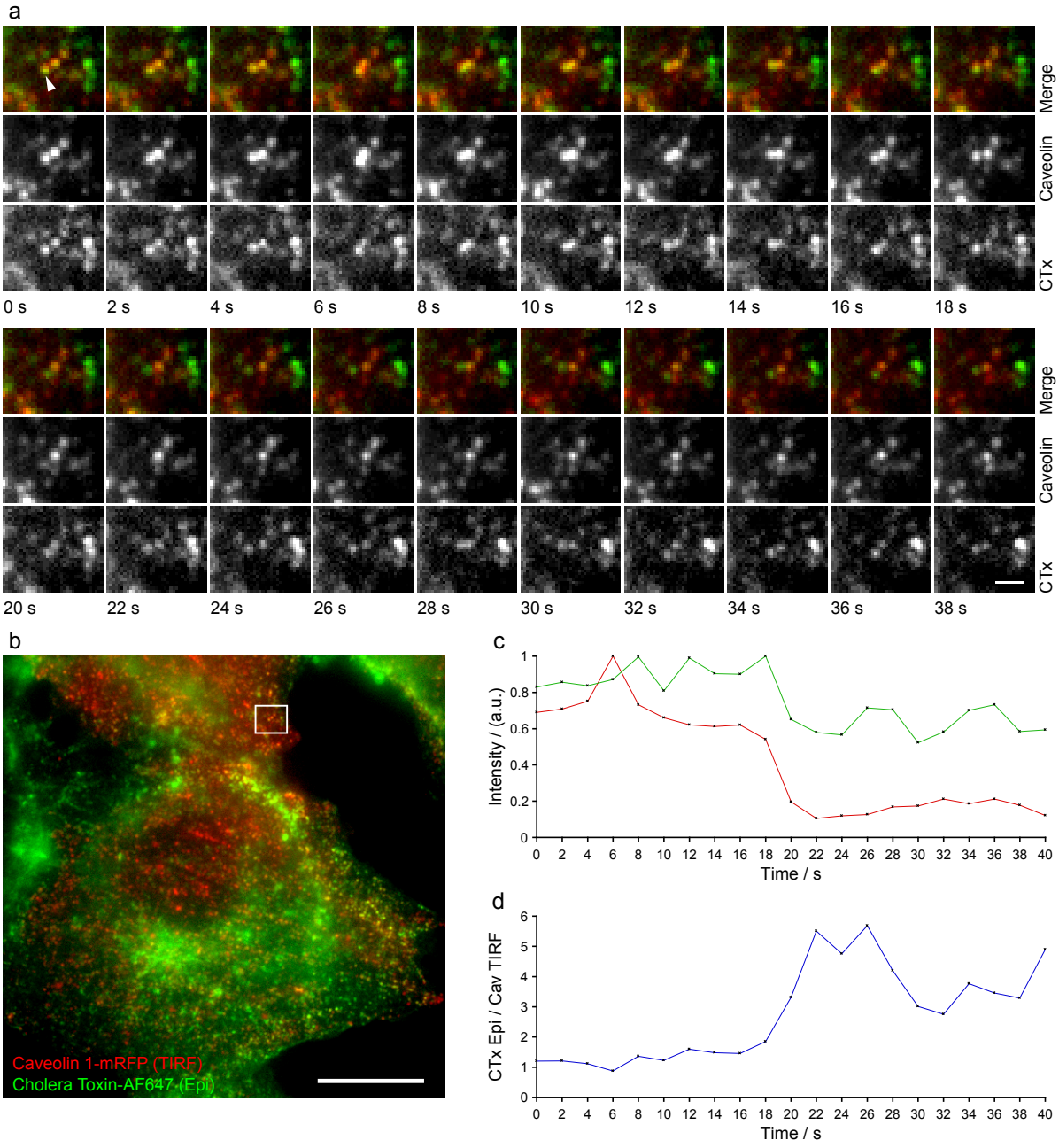

Figure 14: Caveolar internalization of cholera toxin. CV1 cells expressing Caveolin 1-mRFP (Cav1-mRFP) and PH-PLC-EGFP incubated with cholera toxin subunit B-AF647 (CTx-AF647). (a) Cav1-mRFP imaged by TIRF microscopy (middle) and CTx-AF647 under epifluorescence illumination (bottom). The top row shows the merged images with the Cav1-mRFP (TIRF) signal in red and the CTx-AF647 (Epi) signal in green. The caveola dims by moving out of the evanescent field whereas the CTx-AF647 (Epi) signal stays. (b) Overview of the merged images. (c) Fluorescence intensity of Cav1-mRFP (TIRF) in red and CTx-AF647 (Epi) in green plotted against time. The measured signals were normalized. (d) The CTx-AF647 (Epi) trace (c) divided by the Cav1-mRFP (TIRF) trace (c). The Epi to TIRF ratio increases as the caveolae internalizes. Scale bars represent 0.8 μm (a) and 10 μm (b).

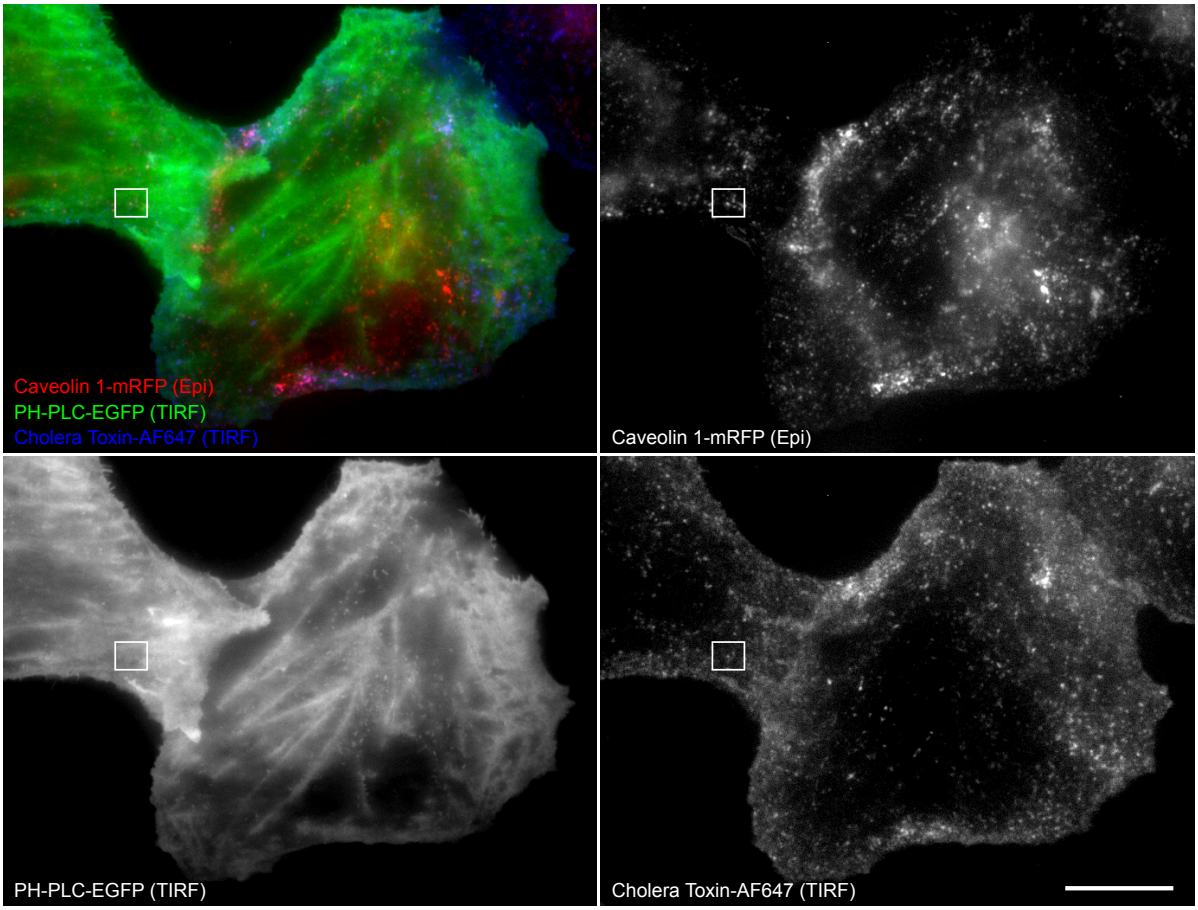

Figure 15: Localization of cholera toxin in caveolin 1-mRFP expressing CV1 cells. Transfected cells were incubated with cholera toxin B-AF647 and examined with the TIRF microscope. Caveolin 1-mRFP was recorded under epifluorescence illumination, while PH-PLC-EGFP and cholera toxin B-AF647 were excited by TIR illumination. The white box surrounds a caveolae loaded with cholera toxin B-AF647 imaged at higher magnification in Figure 16. Scale bar represents 10 μm.

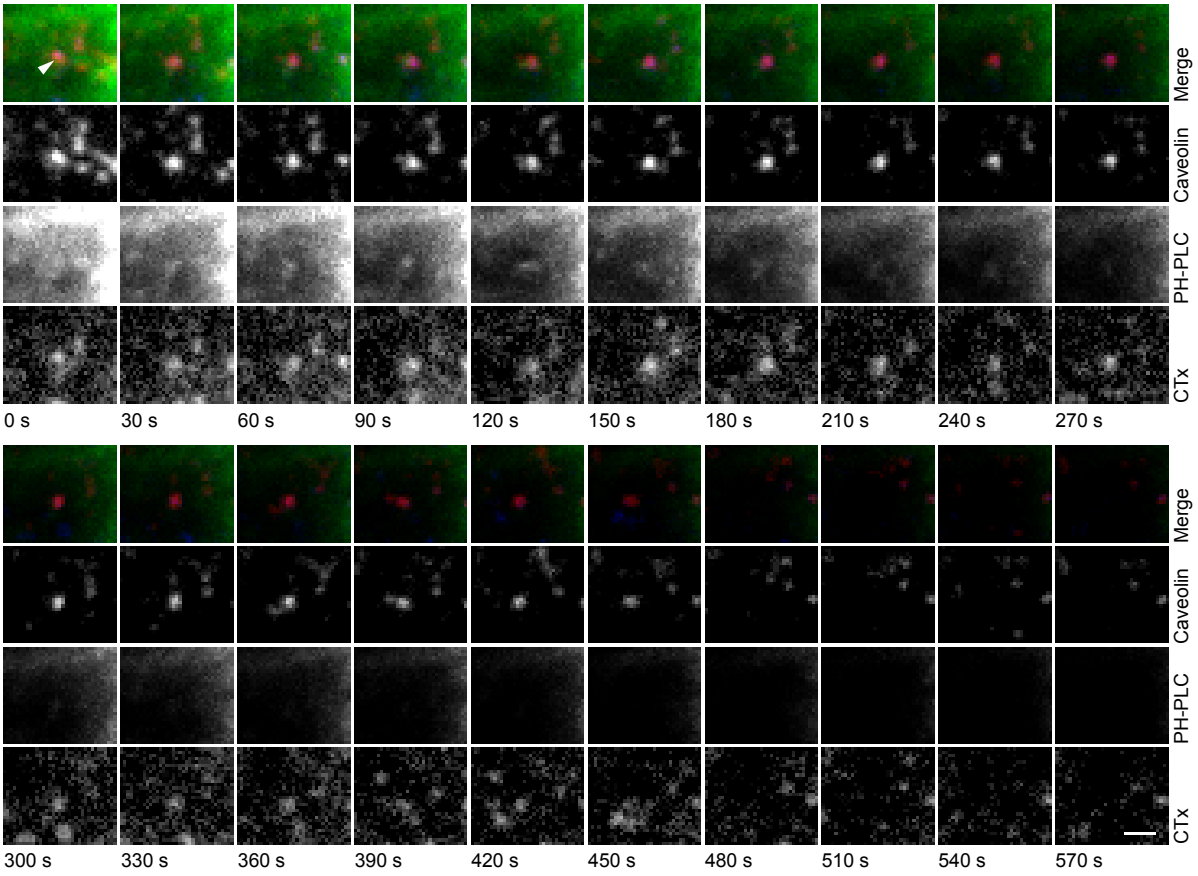

Figure 16: The PH domain of PLC-δ localizes to cholera toxin-loaded caveolae. Expanded views of the white box from Figure 15 are displayed. A time sequence of caveolin 1-mRFP excited by epifluorescence illumination at 568 nm is shown in the second row. PH-PLC-EGFP under TIR illumination at 488 nm is displayed in the third row. The bottom row presents cholera toxin B-AF647 excited by an evanescent field caused by a laser with a wavelength of 647 nm. The top row shows the merged image sequence of all three channels. Scale bar represents 0.8 μm.

4 Discussion

In this work, we have investigated the endocytic internalization of caveolae in high time resolution by the use of TIRF microscopy in live cells. The imaging was complemented by the development of computer programs to yield quantitative data from acquired live cell movies. Taken together, this allowed us to yield the time constant for internalization of caveolae from measurements of the decay in fluorescence intensity of caveolae leaving the evanescent field.

Dual-color TIRF imaging of caveolin 1-mRFP together with GFP-labeled marker proteins was performed to identify cofactors involved in the internalization of caveolae. The factors were chosen by educated guess from a list of proteins that are known to act in clathrin-mediated endocytosis or that have been found to interact with caveolin 1 either *in vivo* and/or *in vitro*.

While several of these factors proved to interact with internalizing or mobile caveolae, none was involved in every individual internalization event we imaged. We can therefore not conclude to the requirement of any of these factors in caveolar endocytosis. Nevertheless our study has been successful in providing the tools and expertise for future studies.

4.1 Time Resolution of Caveolae Internalization

We found that caveolae disappear from the plasma membrane with a time constant $\tau = 0.4\,\mathrm{s}$. This is much faster than observed for clathrin-coated structures which require 30–60 s to retreat 100 nm from the plasma membrane [4]. The velocity of a retreating clathrin-coated stucture was calculated to approximately 4 nm/s. Unfortunately, we cannot calculate the retreating velocity for caveolae, because we do not know the angle of incidence of the laser beam which causes the evenescent field. Therefore, it is not possible to determine the exact depth of the evanescent field.

4.2 Caveolae and the Actin-Based Endocytic Machinery

When we investigated the role of the actin-based machinery in caveolar endocytosis by colocalization studies of caveolin 1-mRFP with EGFP-actin, Arp3-EGFP and cortactin-EGFP, we found that all examined proteins could be transiently recruited to caveolae in agreement with a postulated role of actin polymerization during caveolar endocytosis. However, in each individual experiment, only few colocalization events were observed. These occurred on stationary and slowly laterally moving caveolae. We also found colocalization at apperearing and disappearing caveolae, but these might be caveolar vesicles that come into the evanescent field and do not fuse with the plasma membrane. The observed proteins of the actin machinery may belong to actin tails related to those described for the intracellular parasites *Listeria* and *Shigella*, clathrin-mediated endocytosis, vaccinia virus and SV40-induced caveolar endocytosis.

In the case of EGFP-actin, the prominent actin stress-fibers might have overlapped with colocalization events so that they were not detectable. Arp3-EGFP staining was

very weak in our cells, so that we cannot draw a quantitative conclusion from the present dataset. Cortactin-EGFP staining was located to clearly distinguishable discrete spots and showed frequent colocalization with caveolae that either internalized or seemed to shuttle within close vicinity of the plasma membrane. That the cortactin-EGFP signal fluctuated either in phase or in opposite phase to caveolin-mRFP signal might reflect a role of cortactin in mediating shuttling of caveolae through the cortical actin network. This way, cortactin would localize either distally or proximally to the plasma membrane in respect to the shuttling caveolae and thus be in or out of phase with caveolin 1-mRFP fluorescence signal.

4.3 Signaling in Caveolar Endocytosis

Examination of cells expressing dynamin 2-EGFP and caveolin 1-mRFP revealed that dynamin can be associated with stationary, but also with laterally moving caveolae. Strinkingly, we found comparably little colocalization with dynamin 2, while immunofluorescence confocal microscopy using antibodys against dynamin and caveolin showed extensive colocalization at the cell surface [18].

By a genome-wide screen of human kinases involved in caveolar endocytosis [1], several kinases acting on the membrane were found. When we examined tyrosine phosphorylation on caveolae using the phosphotyrosine binding YFP-dSH2 construct and caveolin 1-mRFP, we found few caveolae that had colocalizing YFP-dSH2. Due to the strong YFP-dSH2 fluorescence, which is also further in the red region of the spectrum compared to EGFP, we had to carefully rule out bleed through from this construct into the mRFP channel. Both fast moving and stationary caveolae showed YFP-dSH2 fluoresence, but no cointernalization could be observed. We conclude that tyrosine phosphorylation detected by this construct does not seem to be directly linked to endocytosis of caveolae.

Analysis of GFP-Grb2, a phosphotyrosine binding adaptor protein and caveolin 1-mRFP showed a diffuse cloud of GFP-Grb2 around few caveolae. These clouds continuously changed their shape. The changes in shape of GFP-Grb2 stained areas might reflect local reorganization of the actin meshwork around caveolae. The caveolae within these GFP-Grb2 positive areas oscillated in intensity, which in agreement with the cortactin data leads to the conclusion, that caveolae can activate multiple proteins, which facilitate their shuttling through the cortical actin meshwork. However, the sequence of events remains to be investigated. Coimaging of fluorescent protein constructs of cortactin and Grb2 with internalizing caveolae visualized via a far red fluorescent ligand will provide further insight into this problem.

Phosphatidylinositol-4,5-bisphosphate is a major signaling molecule in the cytosolic leaflet of the plasma membrane. Local production of this molecule leads to spatial enrichment and thereby higher affinity for PH-domian containing adaptor and multiplication proteins. We investigated local production of PIP_2 in caveolae by double-transfection of cells with PH-PLC-EGFP and caveolin 1-mRFP. In contrast to all other previously analyzed proteins, we found multiple spots with colocalizing caveolin 1-mRFP and PH-PLC-EGFP. Most of these spots were located very close to each other. Because of the

limited spatial resolution, we could not determine whether they were in fact colocalizing spots. It seemed, that PH-PLC-EGFP positive spots were sometimes moving over caveolin 1-mRFP spots, and vice versa. Yet, we found appearing and disappearing caveolae with associated PH-PLC-EGFP. We could not detect any additional recruitment of PH-PLC-EGFP to such colocalizing spots. We can therefore support the finding that caveolae are enriched in PIP_2. But since we could not find any obvious change in the amount of PH-PLC-EGFP associated with internalizing caveolae, we can not conclude to a role of PIP_2 in caveolar endocytosis from our data.

4.4 Internalization of Cholera Toxin

Cholera toxin is a well-described ligand for caveolar endocytosis. We used AF647-labeled cholera toxin B to induce endocytosis and therby specifically label caveolae undergoing endocytosis. Membrane-bound cholera toxin localized to surface caveolae to a high extent and started to cointernalize with caveolae few minutes after binding. We could observe in epifluorescence, that after 30 min a large extent of cholera toxin B-AF647 was internalized to the Golgi complex. This is in agreement with previous studies which reported a half life of 10 min to 2 h depending on the assay [31, 32]. When observing caveolar internalization of cholera toxin B-AF647, we found that the internalization process itself requires only seconds. When cells were first incubated at 4 °C to enable binding of cholera toxin and then shifted to 37 °C, disappearance of surface cholera toxin was detected as early as 10 min after incubation [31]. Therefore, we suggest that the time determinant factor is not the binding of cholera toxin to cells, but the subsequent recruitment of factors required for endocytosis to caveolae. If all factors are in place, internalization can be triggered and cholera toxin-loaded caveolae fission and move into the cell.

In three-color movies of PH-PLC-EGFP, caveolin 1-mRFP and cholera toxin B-AF647, only few triple colocalization spots were present. Therefore, we concluded, that PIP_2 can be enriched in cholera toxin-labeled caveolae, but is not required for endocytosis.

4.5 Future Challenges

In this study, we established quantitative live-cell TIRF microscopy of caveolar endocytosis, and further qualitatively described the role of the actin based machinery and signaling mechanisms in caveolar endocytosis by TIRF microscopy. The investigation of additional interaction partners in ligand-mediated caveolar endocytosis is the next logic target of research. The use of dominant negative mutants of for example dynamin 2 would be a further useful tool. An additional challenge is the development of a triple-color TIRF microscopy technique. This would enable us to simultaneously visualize caveolin 1-mRFP, an GFP-labeled interacting protein and an AF647-labeled ligand during endocytic internalization. To investigate the role of PIP_2 in caveolar endocytosis, we suggest to complement imaging with inhibitor studies.

Acknowledgments

First I would thank Helge for his great supervision and support of my experiments. I would also thank Ari Helenius for giving me the possibility to work in his lab. I would thank Akiko for her patient support on the TIRF microscope and also Jürg and Roland for helping me out on computer problems. Finally I would thank the entire E-floor of the HPM building for additional aid and the nice atmosphere.

References

[1] Lucas Pelkmans, Eugenio Fava, Hannes Grabner, Michael Hannus, Bianca Habermann, Eberhard Krausz, and Marino Zerial. Genome-wide analysis of human kinases in clathrin- and caveolae/raft-mediated endocytosis. *Nature*, May 2005.

[2] Dorothy A Schafer. Coupling actin dynamics and membrane dynamics during endocytosis. *Curr Opin Cell Biol*, 14(1):76–81, Feb 2002.

[3] James D Orth and Mark A McNiven. Dynamin at the actin-membrane interface. *Curr Opin Cell Biol*, 15(1):31–9, Feb 2003.

[4] Christien J Merrifield, Morris E Feldman, Lei Wan, and Wolfhard Almers. Imaging actin and dynamin recruitment during invagination of single clathrin-coated pits. *Nat Cell Biol*, 4(9):691–8, Sep 2002.

[5] Christien J Merrifield, Britta Qualmann, Michael M Kessels, and Wolfhard Almers. Neural Wiskott Aldrich Syndrome Protein (N-WASP) and the Arp2/3 complex are recruited to sites of clathrin-mediated endocytosis in cultured fibroblasts. *Eur J Cell Biol*, 83(1):13–8, Feb 2004.

[6] Defne Yarar, Clare M Waterman-Storer, and Sandra L Schmid. A Dynamic Actin Cytoskeleton Functions at Multiple Stages of Clathrin-mediated Endocytosis. *Mol Biol Cell*, 16(2):964–75, Feb 2005.

[7] Hong Cao, James D Orth, Jing Chen, Shaun G Weller, John E Heuser, and Mark A McNiven. Cortactin is a component of clathrin-coated pits and participates in receptor-mediated endocytosis. *Mol Cell Biol*, 23(6):2162–70, Mar 2003.

[8] MA McNiven, L Kim, EW Krueger, JD Orth, H Cao, and TW Wong. Regulated interactions between dynamin and the actin-binding protein cortactin modulate cell shape. *J Cell Biol*, 151(1):187–98, Oct 2000.

[9] Lucas Pelkmans and Ari Helenius. Endocytosis via caveolae. *Traffic*, 3(5):311–20, May 2002.

[10] S Li, R Seitz, and MP Lisanti. Phosphorylation of caveolin by src tyrosine kinases. The alpha-isoform of caveolin is selectively phosphorylated by v-Src in vivo. *J Biol Chem*, 271(7):3863–8, Feb 1996.

[11] CC Mastick, MJ Brady, and AR Saltiel. Insulin stimulates the tyrosine phosphorylation of caveolin. *J Cell Biol*, 129(6):1523–31, Jun 1995.

[12] Haiming Cao, Amy R Sanguinetti, and Cynthia Corley Mastick. Oxidative stress activates both Src-kinases and their negative regulator Csk and induces phosphorylation of two targeting proteins for Csk: caveolin-1 and paxillin. *Exp Cell Res*, 294(1):159–71, Mar 2004.

[13] Lucas Pelkmans, Daniel Püntener, and Ari Helenius. Local actin polymerization and dynamin recruitment in SV40-induced internalization of caveolae. *Science*, 296(5567):535–9, Apr 2002.

[14] M Stahlhut and B van Deurs. Identification of filamin as a novel ligand for caveolin-1: evidence for the organization of caveolin-1-associated membrane domains by the actin cytoskeleton. *Mol Biol Cell*, 11(1):325–37, Jan 2000.

[15] Billy Tsai, Joanna M Gilbert, Thilo Stehle, Wayne Lencer, Thomas L Benjamin, and Tom A Rapoport. Gangliosides are receptors for murine polyoma virus and SV40. *EMBO J*, 22(17):4346–55, Sep 2003.

[16] D Axelrod. Total internal reflection fluorescence microscopy in cell biology. *Traffic*, 2(11):764–74, Nov 2001.

[17] JA Steyer and W Almers. A real-time view of life within 100 nm of the plasma membrane. *Nat Rev Mol Cell Biol*, 2(4):268–75, Apr 2001.

[18] H Cao, F Garcia, and MA McNiven. Differential distribution of dynamin isoforms in mammalian cells. *Mol Biol Cell*, 9(9):2595–609, Sep 1998.

[19] H Cao, HM Thompson, EW Krueger, and MA McNiven. Disruption of Golgi structure and function in mammalian cells expressing a mutant dynamin. *J Cell Sci*, 113 (Pt 11):1993–2002, Jun 2000.

[20] Niki Scaplehorn, Anna Holmström, Violaine Moreau, Freddy Frischknecht, Inge Reckmann, and Michael Way. Grb2 and Nck act cooperatively to promote actin-based motility of vaccinia virus. *Curr Biol*, 12(9):740–5, Apr 2002.

[21] L Pelkmans, J Kartenbeck, and A Helenius. Caveolar endocytosis of simian virus 40 reveals a new two-step vesicular-transport pathway to the ER. *Nat Cell Biol*, 3(5):473–83, May 2001.

[22] Lucas Pelkmans, Thomas Bürli, Marino Zerial, and Ari Helenius. Caveolin-stabilized membrane domains as multifunctional transport and sorting devices in endocytic membrane traffic. *Cell*, 118(6):767–80, Sep 2004.

[23] Nathalie Sauvonnet, Annick Dujeancourt, and Alice Dautry-Varsat. Cortactin and dynamin are required for the clathrin-independent endocytosis of gammac cytokine receptor. *J Cell Biol*, 168(1):155–63, Jan 2005.

[24] Lucas Pelkmans and Mariano Zerial. Kinase-regulated quantal assembly, kiss-and-run and recycling of caveolae. *Nature*, 2005. In press.

[25] RG Parton, B Joggerst, and K Simons. Regulated internalization of caveolae. *J Cell Biol*, 127(5):1199–215, Dec 1994.

[26] P Oh, DP McIntosh, and JE Schnitzer. Dynamin at the neck of caveolae mediates their budding to form transport vesicles by GTP-driven fission from the plasma membrane of endothelium. *J Cell Biol*, 141(1):101–14, Apr 1998.

[27] JR Henley, EW Krueger, BJ Oswald, and MA McNiven. Dynamin-mediated internalization of caveolae. *J Cell Biol*, 141(1):85–99, Apr 1998.

[28] Qing Yao, Jing Chen, Hong Cao, James D Orth, J Michael McCaffery, Radu-Virgil Stan, and Mark A McNiven. Caveolin-1 interacts directly with dynamin-2. *J Mol Biol*, 348(2):491–501, Apr 2005.

[29] HR Hope and LJ Pike. Phosphoinositides and phosphoinositide-utilizing enzymes in detergent-insoluble lipid domains. *Mol Biol Cell*, 7(6):843–51, Jun 1996.

[30] LJ Pike and L Casey. Localization and turnover of phosphatidylinositol 4,5-bisphosphate in caveolin-enriched membrane domains. *J Biol Chem*, 271(43):26453–6, Oct 1996.

[31] PH Fishman. Internalization and degradation of cholera toxin by cultured cells: relationship to toxin action. *J Cell Biol*, 93(3):860–5, Jun 1982.

[32] D Tran, JL Carpentier, F Sawano, P Gorden, and L Orci. Ligands internalized through coated or noncoated invaginations follow a common intracellular pathway. *Proc Natl Acad Sci U S A*, 84(22):7957–61, Nov 1987.

Appendix

A Abbreviations

AF647	Alexa Fluor 647
AP	adapter protein
Arp3	actin-related protein 3
ATCC	american type culture collection
Cav1	caveolin 1
CCD	charge-coupled device
Cttn	cortactin
CTx	cholera toxin subunit B
D-MEM	Dulbecco's modified Eagle medium
DNA	desoxyribulose nucleic acid
Dyn2	dynamin 2
EDTA	ethylenediaminetetraacetat, $((HOOCCH_2)_2NCH_2)_2$
EGFP	enhanced green fluorescent protein
F-actin	filamentous actin
FCS	fetal calf serum
GFP	green fluorescent protein
GPI	glycosylphosphatidylinositol
Grb2	growth factor receptor bound protein 2
HEPES	4-(2-hydroxylethyl)-1-piperazineethanesulfonic acid
MEM	minimum essential medium
mRFP	monomeric red fluorescent protein
NA	numerical aperture
NEAA	nonessential amino acids
PH	pleckstrin homology domain
PIP_2	phosphatidylinositol-4,5-bisphosphate
PLC	phospholipase C
PRD	proline/arginine-rich domain
RFP	red fluorescent protein
RGB	red green blue
ROI	region of interest
SH2	Src homology 2 domain
SH3	Src homology 3 domain
SV40	Simian virus 40
TIR	total internal reflection
TIRF	total internal reflection fluorescence
WASP	Wiskott-Aldrich syndrome protein
YFP	yellow fluorescent protein

B Source Code of Programs

B.1 Step Measure

```
import ij.*;
import ij.process.*;
import ij.gui.*;
import java.awt.*;
import ij.plugin.*;

/** This plugin sets the options of measurements so that
    traceable measuments can be recorded. It then measures
    the current region of interest (ROI) and subsequently
    moves to the next slice.
    rolf suter, 2005
 */

public class Step_Measure implements PlugIn {

   public void run(String arg) {
      IJ.run("Set Measurements...",
             "area mean min bounding display redirect=None decimal=3");
      IJ.run("Measure");
      IJ.run("Next Slice [>]");
   }

}
```

B.2 Tracer

```
import ij.*;
import ij.process.*;
import ij.gui.*;
import ij.io.*;
import java.awt.*;
import java.io.*;
import ij.plugin.*;
import java.util.*;   // StringTokenizer

/** This plugin reads the position data of ROIs in the measuring
    results table stored into a text file. Then the plugin
    measures the same regions of interest (ROI) as specified in
    the file. In order to read the position data they have to be
    recorded and stored in the results table. This can be
    achieved by enabling "Bounding Rectangle" in
    "Set Measurements..." in the "Analyse" menu of ImageJ. The
    type of the ROI (rectangular or circular) has to be
    specified manually. The default value is set to circular.
    This plugin can also measure a manually specified
    ROI through an image stack.
    rolf suter, 2005
 */

public class Tracer_ implements PlugIn {
   int              labelCategory = 0;
   int              labelXROI = 0;
   int              labelYROI = 0;
   int              labelWidth = 0;
   int              labelHeight = 0;
   int              labelSlice = 0;

   int              iXROI = 0;
   int              iYROI = 0;
   int              iWidth = 0;
   int              iHeight = 0;
   int              iSlice = 0;
   int              iFirstSlice = 0;
   int              iLastSlice = 0;

   ImagePlus         imp;
   boolean           bAbort;
   static boolean    manual;
```

```
static boolean   oval;
static boolean   centered;
static boolean   draw;

String[][]       track = new String[2000][50];
   // defines the array where the data from the text file
   // are stored. This defines the maximal number of
   // data point that can be read from the file.



public void run (String arg) {
   imp = WindowManager.getCurrentImage();
   dialog();

   if (draw)
      IJ.setForegroundColor(255, 255, 255);
   if (manual) {
      iSlice = iFirstSlice;
      while (iSlice <= iLastSlice) {
         setRoi(imp);
         IJ.run("Measure");
         if (draw)
            IJ.run("Draw");
         iSlice++;
      }
   }
   else {
      initTrack(track);
      readTrack(track);

      traceTrack(imp, track);
   }


}


public void traceTrack(ImagePlus ip, String[][] array) {
   int measurement = 0;
   int category = 0;

   while(array[0][category] != "?"){
         // reads the label and defines in
```

```
      // which columns the variables are

   if (array[0][category].equals("Label"))
      labelSlice = category;
         // finds the column which defines
         // the slice number of the ROI


   if (array[0][category].equals("BX"))
      labelXROI = category;
         // finds the column which defines
         // the x-coordinate of the ROI

   if (array[0][category].equals("BY"))
      labelYROI = category;
         // finds the column which defines
         // the y-coordinate of the ROI

   if (array[0][category].equals("Width"))
      labelWidth = category;
         // finds the column which defines
         // the width of the ROI

   if (array[0][category].equals("Height"))
      labelHeight = category;
         // finds the column which defines
         // the height of the ROI

   category++;
}

measurement++;

while(array[measurement][1] != "?") {
      // loop over all measurements


   int labelNumberFirstPos =
      array[measurement][labelSlice].lastIndexOf(":")+1;
       // extracts the slice number from the slice label

   int labelNumberLastPos  =
      array[measurement][labelSlice].length();
```

```
      String labelNumber = array[measurement][labelSlice].substring(
               labelNumberFirstPos, labelNumberLastPos);

      iSlice  = Integer.parseInt(labelNumber);
         // first slice number is 1!

      iXROI   = Integer.parseInt(array[measurement][labelXROI]);
      iYROI   = Integer.parseInt(array[measurement][labelYROI]);
      iWidth  = Integer.parseInt(array[measurement][labelWidth]);
      iHeight = Integer.parseInt(array[measurement][labelHeight]);

      setRoi(ip);
      IJ.run("Measure");
      if (draw)
         IJ.run("Draw");

      measurement++;
   }


}


public void showTrack(String[][] array) {
   int zeilenLaenge = array.length;
   int spaltenLaenge = array[0].length;

   for(int zeile = 0; zeile < zeilenLaenge; zeile++)
      for(int spalte = 0; spalte < spaltenLaenge; spalte++)
         {
         IJ.showMessage(array[zeile][spalte]);
         }
}


public void initTrack(String[][] array) {
   int zeilenLaenge = array.length;
   int spaltenLaenge = array[0].length;

   for(int zeile = 0; zeile < zeilenLaenge; zeile++)
      for(int spalte = 0; spalte < spaltenLaenge; spalte++)
         array[zeile][spalte] = "?";
}
```

```
public void readTrack(String[][] array) {
   OpenDialog od = new OpenDialog("Input File", null);
   String name = od.getFileName();

   if (name==null)
      return;
   String dir = od.getDirectory();

   try {

      BufferedReader r = new BufferedReader(new FileReader(dir+name));
      String zeile = "";
      String text  = "";
      int measurement = 0;

      while ((zeile = r.readLine()) != null) {
         StringTokenizer tokens = new StringTokenizer(zeile, " ");
            // Tokens are separated by Tabs

         int i = 0;

         while (tokens.hasMoreTokens() ) {
            String element = "";
            array[measurement][i] = tokens.nextToken();
            i++;
         }

         measurement++;
      }

      r.close();
      }

      catch (IOException e) {
         IJ.error(""+e);
         return;
   }

}


public void dialog() {
```

```
   oval        = true;
   manual      = false;
   centered    = false;
   draw        = false;
   iFirstSlice = imp.getStackSize();
   iLastSlice  = iFirstSlice;

   GenericDialog gd = new GenericDialog
      ("Tracer Input", IJ.getInstance());

   gd.addCheckbox("Oval Areas", oval);
   gd.addCheckbox("Centered Areas", centered);
   gd.addCheckbox("Manually specified ROIs:",manual);
   gd.addNumericField("Width:", iWidth, 0);
   gd.addNumericField("Height:", iHeight, 0);
   gd.addNumericField("X Coordinate:", iXROI, 0);
   gd.addNumericField("Y Coordinate:", iYROI, 0);
   gd.addNumericField("First Slice:", iFirstSlice, 0);
   gd.addNumericField("Last Slice:", iLastSlice, 0);
   gd.addCheckbox("Draw ROI", draw);
   gd.showDialog();

   if (gd.wasCanceled()) {
      bAbort = true;
      return;
   }

   oval        = gd.getNextBoolean();
   centered    = gd.getNextBoolean();
   manual      = gd.getNextBoolean();
   iWidth      = (int) gd.getNextNumber();
   iHeight     = (int) gd.getNextNumber();
   iXROI       = (int) gd.getNextNumber();
   iYROI       = (int) gd.getNextNumber();
   iFirstSlice = (int) gd.getNextNumber();
   iLastSlice  = (int) gd.getNextNumber();
   draw        = gd.getNextBoolean();

}


public void setRoi(ImagePlus ip) {
   int iX;
   int iY;
```

```
            // test if user wants coordinates to be in center of ROI
        if (centered) {
            iX = iXROI - (iWidth/2);
            iY = iYROI - (iHeight/2);
        }
        else {
            iX = iXROI;
            iY = iYROI;
        }

            // test if user wants oval
        if (oval)
            ip.setRoi(new OvalRoi(iX,iY, iWidth, iHeight, ip));
                // draws an oval ROI
        else
            ip.setRoi(iX, iY, iWidth, iHeight);
                // draws a rectangular ROI

        int stacksize = ip.getStackSize();

            // test if the slice fulfills the requirements
        if (iSlice > 0 && iSlice <= stacksize) {
            ip.setSlice(iSlice);
            ip.repaintWindow();
        }

    }
}
```